Modeling CCN activity of chemically unresolved aerosol, including surface tension, non-ideality, and bulk/surface partitioning

Nønne L. Prisle[1,2]

[1]University of Oulu, Nano and Molecular Systems Research Unit, P.O. Box 3000, 90014, University of Oulu, Finland
[2]University of Helsinki, Department of Physics, P.O. Box 48, 00014, University of Helsinki, Finland

Correspondence: N. L. Prisle
(nonne.prisle@oulu.fi)

Abstract. We present a thermodynamically consistent framework that enables self-contained, predictive Köhler calculations of droplet growth and activation with considerations of surface adsorption, surface tension reduction, and non-ideal water activity for chemically unresolved, complex surface active aerosol mixtures. The common presence of surface active components in atmospheric aerosols is now well-established, whereas the role of different mechanisms driven by surface activity in aerosol hygroscopic growth and cloud droplet activation remains to be fully constrained. Because specific characterization of key properties, such as water activity and surface tension, are challenging to obtain directly for finite-sized activating droplets, a robust model framework is needed to gain further insight into the droplet equilibrium growth process. The present model couples Köhler theory with the Gibbs adsorption and Szyszkowski-type surface tension equations and is formulated on a mass-basis to allow for a quantitative description of chemically unresolved mixtures. The model is applied to calculate cloud condensation nuclei (CCN) activity of aerosol particles comprising Nordic Aquatic Fulvic Acid (NAFA), a strongly surface active model atmospheric humic-like substance (HULIS), and NaCl with dry diameters of 30–230 nm and compositions spanning the full range of relative NAFA and NaCl mixing ratios. Parametrizations of aqueous surface tension and water activity with respect to independently varying NAFA and NaCl mass concentrations were developed to obtain continuous descriptions of non-ideal interactions governing both bulk and surface properties during droplet growth and activation. Effects of NAFA surface activity are gauged *via* a suite of properties evaluated for growing and activating droplets and results are compared to those of several other predictive Köhler frameworks, where surface active components in droplet solutions are considered in different ways. Throughout droplet growth and activation, the finite amounts of surface active material in microscopic and submicron droplets are strongly depleted from the bulk phase due to bulk/surface partitioning, because surface areas for a given bulk volume are very large. As a result, both surfactant strength and hygroscopicity of NAFA is predicted to be significantly lower in finite-sized activating droplets than in macroscopic aqueous solutions of the same overall composition. The influence of surface activity on CCN activation of the complex NAFA mixture is therefore very similar to what has previously been found for simple, strong surfactants and well represented by the Gibbs adsorption framework.

1 Introduction

The surface activity of atmospheric aerosol components and its implications for cloud microphysics have been investigated for several decades. By definition, surface active (surfactant) material adsorb at the surface of a solution, leading to enhanced surface concentrations (activity), compared to the (interior) bulk, and a resulting radial concentration gradient between the surface and bulk phases. Due to this enhanced surface activity, surfactants can typically reduce surface tension of aqueous solutions more efficiently at a given concentration than homogeneously mixed solutes. Shulman et al. (1996) showed that reduced surface tension in aqueous droplets can alter the shape of their equilibrium growth curve as described by Köhler theory (Köhler, 1936) and thereby lower the critical supersaturation threshold for cloud droplet activation. Facchini et al. (1999, 2000) then demonstrated that surface active material is indeed present in atmospheric cloud and fog samples, which can significantly reduce aqueous surface tension at concentrations comparable to those of activating droplets. Surface active components have now been found in atmospheric aerosols from many different environments (e.g. Petters and Petters, 2016; Gérard et al., 2016; Kroflič et al., 2018).

To describe the evolving state of a growing droplet, Köhler calculations generally require composition-dependent droplet properties in some form. The surface equation-of-state for a solution can be given in terms of either the surface or bulk composition, as these quantities are related *via* the equilibrium bulk-to-surface concentration gradient for a given surface active substance. A number of techniques exist to experimentally determine the surface tension–composition relations for surfactant solutions, which almost exclusively require macroscopic (i.e. millimeter-scale or larger) sample sizes (Fainerman et al., 2002; Hyvärinen et al., 2006; Vanhanen et al., 2008; Alvarez et al., 2010; Kristensen et al., 2014; Bzdek et al., 2020). In these macroscopic solutions, the bulk phase can be considered an infinite reservoir, compared to the finite surface phase. Surface adsorption and enhanced surface activity therefore involve only a small fraction of the total amount of surface active solute and have negligible effect on the bulk composition. As a consequence, surface tension–composition relations reported in terms of total solute concentrations, which are readily constrained experimentally for macroscopic solutions, closely reflect the corresponding bulk composition.

In microscopic and sub-micron activating cloud droplets, both surface and bulk phases are finite and the surface area (A) to bulk volume (V) ratio may be orders of magnitude greater than for macroscopic solutions (Prisle et al., 2010; Lin et al., 2020). For example, a spherical droplet with diameter $d = 1$ μm has $A/V = 6/d = 6 \times 10^6$ m^{-1}, whereas $A/V = 6000$ m^{-1} for a macroscopic droplet with $d = 1$ mm. Because the finite-sized droplets comprise finite total amounts of surface active solute, surface adsorption can therefore significantly deplete the droplet bulk phase. Furthermore, the highly sensitive variation of A/V with finite solution size introduces a size-dependent shift in both surface and bulk concentrations of the surface active species at the adsorption equilibrium.

The distribution of surface active species between the distinct bulk and surface phases of a solution is referred to as the bulk/surface *partitioning*. Size-dependent partitioning has been predicted to in turn result in size-modulated composition-dependent properties for finite-sized solution droplets (Bianco and Marmur, 1992; Laaksonen, 1993; Sorjamaa et al., 2004; Prisle et al., 2010), including surface tension (a surface property) and water activity (a bulk property), which are key parameters in determining aerosol water uptake, hygroscopic growth and cloud droplet activation. Until recently, experimental evidence for this effect in cloud microphysics has been indirect, from the reported inability of Köhler models using macroscopic solution property–composition relations to reproduce observed microscopic droplet activation. For example, a range of studies have consistently demonstrated that using surface tension and water activity relations based on total solution composition, without explicit consideration of the impact of surface adsorption on bulk composition, can lead to dramatic over-estimations of cloud condensation nuclei (CCN) activity (Li et al., 1998; Sorjamaa et al., 2004; Prisle et al., 2008, 2010; Kristensen et al., 2014; Hansen et al., 2015; Petters and Petters, 2016; Lin et al., 2018; Forestieri et al., 2018; Prisle et al., 2019). Although previous work has measured the surface tension of micron-sized droplets or air bubbles suspended in a macroscopic surfactant solution medium (e.g. Jin et al., 2004; Alvarez et al., 2010), depletion of the bulk phase from surface adsorption is not significant in these conditions, as the bulk phase can be considered infinite. Bzdek et al. (2020) presented measurements of concentration dependent surface tensions for finite-sized, surfactant-containing aqueous droplets suspended in air, which were significantly higher than those of macroscopic solutions with identical total compositions. These results provided the first direct experimental evidence for the influence of bulk-phase depletion from size-dependent bulk/surface partitioning on the air–solution surface tension of microscopic droplets.

Effects of surfactant bulk/surface partitioning may greatly impact predictions of the cloud forming potential of surface active aerosol (Laaksonen, 1993; Li et al., 1998; Sorjamaa et al., 2004). In Köhler calculations, macroscopic solution property–composition relations are connected to those of growing droplets with changing A/V *via* a partitioning model, which is typically based on a suitable adsorption isotherm and surface tension equation of state for the surface active components. An overview of the most widely used partitioning models in Köhler modeling is given by Malila and Prisle (2018). Thermodynamic process models, such as those presented by Prisle et al. (2010), Topping (2010), Raatikainen and Laaksonen (2011), Petters and Kreidenweis (2013), Ovadnevaite et al. (2017), and Malila and Prisle (2018), generally rely on input of compound-specific properties with well-characterized composition dependencies. Due to the challenges involved in obtaining sufficient amounts of atmospheric samples and characterizing their composition and composition-dependent properties in aqueous solution, including surface activity (e.g. Kroflič et al., 2018; Prisle et al., 2019), many process-level experimental and modeling studies have used sodium dodecyl sulfate (SDS) and similar industrial surfactants with relatively well-known properties as model compounds for surface active components of real atmospheric aerosols (e.g. Li et al., 1998; Sorjamaa et al., 2004; Harmon et al., 2010; Prisle et al., 2011; Raatikainen and Laaksonen, 2011; Petters and Kreidenweis, 2013).

The first atmospheric surfactants used in Köhler calculations together with a thermodynamic partitioning model were straight-chain fatty acid sodium salts (Prisle et al., 2008, 2010, 2011; Forestieri et al., 2018), which are widely identified in atmospheric aerosol samples (e.g. Yassaa et al., 2001; Mochida et al., 2002, 2003; Cheng et al., 2004). Both SDS, fatty acids, and their salts are relatively strong surfactants, yet the modeled effect of surface tension on CCN activation was very modest, due to strong depletion of the surfactant molecules from the bulk phase in activating droplets arising from surface partitioning. Overall, these model predictions reproduced experimental observations of CCN activity well. The atmospherically relevant surfactants so far studied in terms of detailed compound-specific solution properties (see e.g. overview by Petters and Petters, 2016) comprise a relatively narrow selection of often simple, homologous molecules, which most likely do not represent the properties of all atmospheric surface active compounds. Furthermore, the binary and ternary aqueous droplet mixtures which are typically the focus of process-level studies may constitute too simple proxy systems to capture the variation of properties displayed by chemically complex surface active aerosol mixtures in the atmosphere. Significant variation in aerosol surface activity may be reflected in the somewhat diverging messages regarding the importance of surface tension for closure of CCN activity and number concentrations from different studies (e.g. Wex et al., 2007; Varga et al., 2007; Asa-Awuku et al., 2008; George et al., 2009; Booth et al., 2009; Poulain et al., 2010; Frosch et al., 2011; Ovadnevaite et al., 2017).

Atmospheric aerosol samples, as well as those generated in more elaborate laboratory experiments, often comprise complex mixtures which are chemically either partially or entirely unresolved. A major challenge in establishing general results for the role of surface active aerosol in cloud microphysics relates to the composition-dependent thermodynamic description and process modeling of such chemically diverse and unresolved aerosol mixtures. Even in the hypothetical case where all aerosol components and their quantities would be known, it is often not realistic to obtain a well-constrained description of their interactions in all solution states corresponding to growing and activating droplets. To enable predictive calculations, one approach is to assume a well-known proxy compound or mixture to represent the properties of the complex system (Prisle et al., 2012a; Ovadnevaite et al., 2017; Lowe et al., 2019). A key challenge of this approach concerns how representative the chosen proxy system is of the actual aerosol mixture and in particular how well the proxy represents responses of the actual mixture to varying conditions. Alternatively, Prisle et al. (2011) proposed a very simple framework for representing the overall effect of aerosol surface activity on CCN activation. This model rather crudely assumes that surface active components are completely partitioned to the droplet surface with a resulting effective hygroscopicity parameter of $\kappa = 0$ (Petters and Kreidenweis, 2007) and vanishing impact on droplets surface tension. It can therefore readily be applied to any surface active aerosol, including chemically unresolved mixtures. The simple representation was demonstrated to perform well for SDS and fatty acid salts with 8–12 carbon atoms ($\mathrm{C}_8, \mathrm{C}_{10}, \mathrm{C}_{12}$), but the general applicability to complex surface active aerosol mixtures remains to be established.

Here, we present a framework that enables predictive, thermodynamically consistent calculations of droplet growth and activation for chemically unresolved, complex surface active aerosol mixtures. Following the approach of Prisle et al. (2010), Köhler theory is coupled with a partitioning model based on the Gibbs adsorption and Szyszkowski-type surface tension equations. To allow for a quantitative description of chemically unresolved components, the model is formulated on a mass-basis and continuous parametrizations for bulk water activity and surface tension in aqueous solutions are constructed from macroscopic measurements, where composition-dependency is described in terms of mass-concentrations without specific knowledge of the molecular identity of all solute components.

The model is applied to evaluate a suite of properties, including critical supersaturation and droplet size, bulk-phase composition, water activity, surface tension and Kelvin effect, for growing and activating droplets formed from particles comprising Nordic Aquatic Fulic Acid (NAFA) mixed with sodium chloride (NaCl). NAFA is one of several commercial reference compounds used as models for atmospheric HUmic LIke Substances (HULIS), which comprise another major group of atmospheric surface active organics (e.g. Kiss et al., 2005; Dinar et al., 2006b; Graber and Rudich, 2006). Kristensen et al. (2014) and Lin et al. (2020) report a comprehensive data set, including measurements of CCN activity for particles with a range of sizes comprising NAFA and NaCl in various mixing ratios, as well as surface tension and water activity for a large set of macroscopic aqueous NAFA–NaCl solutions with different relative solute mixing ratios and concentrations. NAFA significantly reduces surface tension in macroscopic aqueous solutions, similar to other model HULIS (e.g. Kiss et al., 2005; Aumann et al., 1967). However, Kristensen et al. (2014) found that CCN activity of both pure NAFA and mixed NAFA–NaCl particles was significantly overestimated by Köhler calculations assuming the impact of NAFA surface activity on droplet surface tension to be equivalent to that measured in the corresponding macroscopic solutions. This strongly suggests that size-dependent bulk/surface partitioning of NAFA in microscopic droplets also needs to be taken into account to explain the observed CCN activity.

2 Theory and modeling

CCN activity for NAFA particles of varying dry sizes and mixing ratios with NaCl was calculated using a framework based on the Köhler equation in the form (Köhler, 1936; Prisle et al., 2010)

$$\frac{SS}{[100\%]} \equiv \frac{p_\mathrm{w}}{p_\mathrm{w}^0} - 1 = a_\mathrm{w} \exp\left(\frac{4\sigma\nu_\mathrm{w}}{RTd}\right) - 1\,. \tag{1}$$

Equation 1 describes the equilibrium water vapor supersaturation (SS) over a spherical solution droplet as a function of its diameter (d): p_w is the equilibrium partial pressure of water over the solution droplet, p_w^0 is the saturation vapor pressure over a planar surface of pure water, a_w and σ are the water activity and surface tension of the droplet solution, ν_w is the partial molar volume of water in solution, approximated as the ratio of pure water molar mass and mass density $M_\mathrm{w}/\rho_\mathrm{w}$, R is the universal gas constant, and T is the Kelvin temperature.

The solution droplet is formed as water condenses onto an initially dry particle. Only the dry particle itself, before any water uptake has occurred, is here referred to as a "particle" and dry particle diameters (as well as other properties) are designated in upper case symbols, as D_p. After water uptake, the wet aerosol particle is referred to as a (solution) droplet, and corresponding diameters (and other properties) are designated in lower case symbols, as d. For each dry particle size and composition, the critical supersaturation (SS_c) is evaluated as the maximum of the equilibrium droplet growth (Köhler) curve described by Eq. 1. The droplet size where SS_c occurs is here referred to as the critical droplet diameter d_c, or the *point of activation*. When droplets have grown past their respective critical point to sizes $d > d_\mathrm{c}$, they are described as *activated* cloud droplets. At earlier points $d \leq d_\mathrm{c}$ on the Köhler curves, droplets are considered to be in the process of *activating*.

The water activity (also called the Raoult term) describes the suppression of equilibrium water partial pressure over an aqueous solution by dissolved solutes, compared to the saturation vapor pressure of pure water, as

$$p_\mathrm{w} = a_\mathrm{w} p_\mathrm{w}^0 = \gamma_\mathrm{w} x_\mathrm{w} p_\mathrm{w}^0\,. \tag{2}$$

Here, x_w is the water (mole or mass) fraction in solution and γ_w is the corresponding (mole or mass fraction based) activity coefficient of water. The exponential (or Kelvin) term describes the enhancement of vapor pressure over the convex side of a curved droplet surface, compared to a planar surface of the same liquid, and depends explicitly on the droplet surface tension. Both water activity and Kelvin term are functions of droplet composition, determining x_{w} and thus $\gamma_{\mathrm{w}} = \gamma_{\mathrm{w}}(x_{\mathrm{w}})$ and $a_{\mathrm{w}} = \gamma_{\mathrm{w}} x_{\mathrm{w}}$, as well as any concentration dependent change in droplet solution surface tension from the pure water value, $\Delta\sigma = \sigma_{\mathrm{w}} - \sigma$.

The total (T) amount of solute in the growing droplets remains constant and is determined from the dry particle compositions in terms of relative mass fractions $W_{\mathrm{p},s}$ of each solute component s, where $\sum_s W_{\mathrm{p},s} = 1$. Assuming volume additivity in spherical particles, the total dry mass of each solute component is then given from their bulk mass densities ρ_s as

$$m_s^T = W_{\mathrm{p},s} \frac{\pi}{6} D_{\mathrm{p}}^3 \left(\sum_j \frac{W_{\mathrm{p},s}}{\rho_j} \right)^{-1} . \tag{3}$$

In our calculations, we have used $\rho_{\mathrm{NaCl}} = 2.165\,\mathrm{g\,cm^{-3}}$ and $\rho_{\mathrm{NAFA}} = 1.6\,\mathrm{g\,cm^{-3}}$. In the absence of an exact value, the NAFA density is assumed to be similar to that of Suwannee River Fulvic Acid, another common reference humic substance (Dinar et al., 2006a). The droplet temperature is assumed to be $T = 303$ K, reflecting the range of effective temperatures from about $298 - 313$ K in the CCN counter between measurements at different supersaturations (T.B. Kristensen, personal communication). The sensitivity of calculations to the assumed value of ρ_{NAFA} and variations in experimental droplet temperature is discussed in Section S5 of the Supporting Information (SI).

At each droplet size, the total amount of water is calculated by assuming volume additivity also of water and dry particle components within the droplet phase as

$$m_{\mathrm{w}}^T = \rho_{\mathrm{w}} \frac{\pi}{6} (d^3 - D_{\mathrm{p}}^3) . \tag{4}$$

The total droplet composition $\{x_i^T\} = \mathbf{x^T}$ is then given in terms of the mass fractions of each component $i = (\mathrm{w}, s)$ as

$$x_i^T = \frac{m_i^T}{\sum_j m_j^T} \tag{5}$$

2.1 Bulk/surface partitioning

When surface active material adsorbs at the droplet surface, it leads to a partitioning of the total mass of surface active solute m_{sft}^T between the surface (S) and bulk (B) phases of the solution droplet. This partitioning depletes the droplet bulk concentration, compared to the total concentration $x_{\mathrm{sft}}^B < x_{\mathrm{sft}}^T$, and changes the overall bulk composition $\{x_i^B\} = \mathbf{x^B}$, compared to the total composition of the droplet $\mathbf{x^B} \neq \mathbf{x^T}$. To calculate the resulting amount of solute in the droplet bulk (and surface), we use a partitioning model based on the Gibbs adsorption equation (Gibbs et al., 1928) in the form

$$RT \sum_i \frac{m_i^T}{M_i} \frac{\partial \ln(a_i)}{\partial m_{\mathrm{sft}}^B} + A \frac{\partial \sigma}{\partial m_{\mathrm{sft}}^B} = 0 , \tag{6}$$

where $A = \pi d^2$ is the droplet surface area, m_i^T and M_i are the total and molar mass of each droplet component i, a_i is the activity of each component in the droplet solution, and m_{sft}^B is the mass of surface active (i.e. partitioning) species in the droplet bulk. For chemically well-defined components, here water and NaCl, M_i are well-known quantities. For NAFA, we assume an average molar mass of $\bar{M}_{\mathrm{NAFA}} = 4266\ \mathrm{g\,mol^{-1}}$ according to the experimentally based estimate of Mäkelä and Manninen

(2008). This corresponds to an assumption of the average mass unit of surface active solute partitioning between the bulk and surface of the solution. The sensitivity of calculations to variations in the assumed value of $\bar{M}_{\mathrm{NAFA}}$ is discussed in Section S5 of the SI.

Non-ideal ($a_i \neq x_i$, $\gamma_i \neq 1$) solution effects in the droplets are taken into account *via* the composition-dependent droplet water activity a_{w}, which also enters directly into Eq.1, evaluated from an experimentally-based parameterization as described in Section 2.2 below. Activities for non-volatile solutes are challenging to measure directly, but can in binary solutions be inferred from measurements of the solvent activity *via* the Gibbs-Duhem equation. Since this is not possible for ternary and higher-order mixtures, a_{NAFA} and a_{NaCl} are approximated as the corresponding mass fraction concentrations. Previous estimates for ternary surfactant–NaCl aqueous mixtures showed that this assumption had only minor effects in Köhler calculations (Prisle et al., 2010).

The bulk/surface partitioning equilibrium is solved iteratively from Eq. 6 at each droplet size d and total composition $\mathbf{x}^{\mathbf{T}}$, constrained by mass conservation for all droplet components, $m_i^T = m_i^B + m_i^S$, and by choosing the position of the Gibbs surface to yield the droplet bulk-phase volume equal to the total droplet volume $V = \pi d^3/6$ (Prisle et al., 2010).

2.2 Ternary parametrizations

Iterations of critical supersaturations from Eq.1 require continuous functions for concentration-dependent variations in surface tension and water activity of the growing droplets. Here, both σ and a_{w} are described as functions of the droplet bulk composition $\mathbf{x}^{\mathbf{B}}$, which is the basis for using the Gibbs adsorption equation in the form given in Eq. 6. At equilibrium, the surface and bulk compositions of a given surface active substance are related via the concentration gradient resulting from its surface activity and mass conservation within the solution, just as the activities of water and all other components are by definition the same in all phases of the solution. Although the surface tension of a solution may also be given in terms of the surface composition (Ruehl et al., 2016), a major advantage of using bulk-composition based relations for solution properties is that these can be readily obtained from measurements for macroscopic solutions, where the bulk-phase composition is directly constrained in terms of the total dissolved mass. The absolute surface composition is on the other hand not easily quantified by direct measurement (Prisle et al., 2012b; Werner et al., 2014; Walz et al., 2016, e.g.).

The key to applying composition-dependent properties obtained for macroscopic systems to finite-sized droplets, is to correct the bulk (or surface) concentrations of droplet components according to the changes in bulk/surface partitioning with droplet size. When partitioning of surface active solute to the droplet surface is considered, the bulk concentration changes along the Köhler growth curve in response to both dilution as the droplet grows and changing bulk/surface partitioning, for example expressed in terms of the surface partitioning factor $m_{\mathrm{sft}}^S/m_{\mathrm{sft}}^B$, with changing ratio of the droplet surface area and bulk volume A/V. For ternary water–NAFA–NaCl solution droplets, the relative mass fractions of NAFA and NaCl solute in the droplet bulk phase

$$w_s = \frac{m_s^B}{\sum_j m_j^B}\,, \tag{7}$$

where m_s^B is the mass of solute $s = (\mathrm{NAFA}, \mathrm{NaCl})$ in the droplet bulk and $\sum_s w_s = 1$, therefore change in a continuous fashion from the corresponding dry particle composition given by $W_{\mathrm{p},s}$, as a result of changing NAFA partitioning in the growing droplets. The effect of bulk/surface partitioning is to move the droplet bulk (and surface) phase mixing state in the 2-dimensional NAFA–NaCl concentration domain, compared to the total mixing state of the droplet solution, or to a macroscopic solution with the same composition. As a consequence, continuous parametrizations with respect to independent variations in all component concentrations are needed to evaluate droplet properties over the full range of mixing states realized during droplet growth and activation.

The Köhler and partitioning models are both fully predictive and can in principle be used with any functional form and number of fit parameters used to describe the mass-based composition variation of thermodynamic properties. Parametrizations of both σ and a_{w} were here obtained by fitting continuous functions of NAFA and NaCl aqueous concentrations to the experimental surface tensions and water activities reported by Kristensen et al. (2014) and Lin et al. (2020) for macroscopic solutions with solute compositions similar to the original dry particles, using the least squares method. By using mass-based concentrations, which are readily available from experimental parameters, a quantitative description is obtained for variations in each solution component, including the chemically unresolved NAFA.

2.2.1 Surface tension σ

NAFA–NaCl aqueous surface tensions (in $\mathrm{mN\ m^{-1}}$) were fitted with the Szyszkowski equation in the form (Meissner and Michaels, 1949):

$$\sigma = \sigma_{\mathrm{w}} - q_{\mathrm{st1}} \ln\left(1 + \frac{C_{\mathrm{NAFA}}}{q_{\mathrm{st2}}}\right), \tag{8}$$

where $\sigma_{\mathrm{w}} = 93.6635 + 0.009133\ T - 0.000275\ T^2$ (Dillmann and Meier, 1991; Vanhanen et al., 2008) is the temperature-dependent surface tension of pure water (in $\mathrm{mN\ m^{-1}}$) and C_{NAFA} is the mass concentration of NAFA (in $\mathrm{g\ L^{-1}}$). Dependency of σ on NaCl concentration enters through the fitting parameters q_{st1} and q_{st2}, which are both functions of the relative NAFA–NaCl mass fraction in solution.

Kristensen et al. (2014) and Lin et al. (2020) report that measured aqueous NAFA surface tension decreases with time after formation of the sample surface. This is likely due to both dynamic effects of surface adsorption from diffusion and structural rearrangements in the surface phase, as well as potentially to increasing concentrations of the pendant drop samples from evaporation of water over the course of measurements. Fitting parameters for the surface tension parametrization (Eq. 8) used in the present calculations were obtained from measurement data corresponding to times $t = 600$ s after generation of the pendant drops. Surface equilibration in the microscopic activating cloud droplets is considered to be diffusion controlled (Alvarez et al., 2012) and much faster than for the macroscopic (millimeter-sized) droplets measured with the pendant drop tensiometer (Alvarez et al., 2010). Droplet activation takes place during exposure times of about 1 s in the CCN counter, depending on the particle size and required critical supersaturation (Kristensen et al., 2014). Following the considerations of Prisle et al. (2008), the ratio of the measurement time scales between the pendant drop surface tension measurements corresponding to 600 s and the cloud droplet activation measurements is estimated to be of the same order of magnitude as the ratio of diffusion distances in the samples, given by the diameter ratio of the droplet systems involved in the two types of measurement, i.e. (pendant drop size/activating droplet size)$\sim$(pendant drop measurement time/droplet activation measurement time) $\sim 10^2$–10^3. With this simple argument, any potential dynamic effects related to diffusion of especially the high average molar mass NAFA component to the droplet surface, which could lead to incomplete (non-equilibrium) partitioning of NAFA, are therefore assumed to be at least comparable between the surface tension parametrizations used in our calculations and the droplet activation measurements, if present at all. At the selected time lapse of $t = 600$ s, generally the steepest and the majority of the total dynamic surface tension decrease had occurred in the NAFA–NaCl solutions, indicating that dynamic effects of surface adsorption due to diffusion are limited beyond this point. Because surface tension measurement data corresponding to measurement times of 600 s were available from Kristensen et al. (2014) and Lin et al. (2020) for the widest range of solution compositions, we used these data rather than those corresponding to even longer measurement times. Using a comprehensive set of time-evolving surface tension measurements for aqueous NAFA–NaCl mixtures with a wide range of compositions, Lin et al. (2020) presented a detailed assessment of the effects of time-dependent surface adsorption in Köhler calcuations.

The surface tension fitting parameters q_{st1} (in $\mathrm{mN\ m^{-1}}$) and q_{st2} (in $\mathrm{L\ g^{-1}}$) for times $t = 600$ s are given as

$$q_{\mathrm{st1}} = 10.46 - 4.810\ w_{\mathrm{NAFA}} \tag{9}$$

and

$$q_{\mathrm{st2}} = 0.5947 - 0.3278\ w_{\mathrm{NAFA}}\,, \tag{10}$$

where w_{NAFA} is the (dimensionless) mass fraction of NAFA solute relative to NaCl in the solution bulk phase given in Eq. 7. Fits were made with the constraints that $q_{\mathrm{st1}} \geq 0$ and $q_{\mathrm{st2}} > 0$ for all $w_{\mathrm{NAFA}} \in 0-1$. Goodness of the overall fit to measured surface tensions given by the Sum of Squares Due to Error $\mathrm{SSE} = 78.54$, $\mathrm{R}^2 = 0.9357$, and Root Mean Squared Error $\mathrm{RMSE} = 1.772$.

To investigate the effect of the functional form of the parametrizations used, we also made ternary fits to the surface tension data using the Szyszkowski-type equation given by Prisle et al. (2010), which contains an additional term explicitly including the positive aqueous surface tension gradient with respect to NaCl concentration, as well as having both fitting parameters depend quadratically, instead of linearly, on w_{NAFA}. The more elaborate equations did not significantly improve the fit to macroscopic surface tension data, while introducing several additional fitting parameters to our calculations. We therefore used the simpler Eq. 8 with implicit NaCl dependency and linear variation of the fit parameters with w_{NAFA}.

2.2.2 Water activity a_w

Osmolality-derived water activities were fitted as functions of NaCl and NAFA mass concentrations (C_{NaCl} and C_{NAFA}, both in $\mathrm{g\ L^{-1}}$) in the form:

$$a_{\mathrm{w}} = 1 + q_{\mathrm{a1}} C_{\mathrm{NaCl}} + q_{\mathrm{a2}} C_{\mathrm{NAFA}}\,, \tag{11}$$

with fitting parameters $q_{\mathrm{a1}} = -5.68 \times 10^{-4}\ \mathrm{L\ g^{-1}}$ and $q_{\mathrm{a2}} = -2.68 \times 10^{-5}\ \mathrm{L\ g^{-1}}$. Goodness of the fit given by Sum of Squares Due to Error $\mathrm{SSE} = 1.638 \times 10^{-7}$, $\mathrm{R}^2 = 0.9963$, and Root Mean Squared Error $\mathrm{RMSE} = 6.399 \times 10^{-5}$. Several other, more complex functions were tested as well, but the simple linear relations gave the most reasonable fits to the data over the measured solution composition ranges. Water activities derived from osmometry in principle include all non-ideal solution effects, in particular concentration-dependent NAFA dissociation and effects of any non-ideal interactions among the resulting solute entities (Kiss and Hansson, 2004; Prisle, 2006, e.g.). Still, the linear relationship on mass concentrations of solute with unknown molar content may not be thermodynamically consistent over the entire range of water–NAFA–NaCl mixing states. Indeed, for the limiting case of binary solutions, Eq. 11 does fail to comply with the Gibbs-Duhem relation in the limit of pure NAFA ($m_\mathrm{w} = m_\mathrm{NaCl} = 0$). This state is, however, never realized in our calculations, where droplet growth is initiated at a finite growth factor and tends toward infinite dilution. Zamora and Jacobson (2013) derived water activities from measured hygroscopic growth factors for NAFA–NaCl mixtures and also found near-linear relationships between water activity and total solute (molal) concentration.

2.3 Surfactant representations

Droplet growth and activation is influenced by several simultaneous processes in the aqueous phase, including dilution, partitioning, and non-ideal interactions. To highlight the interplay of different underlying mechanisms, we compare Köhler calculations using the full mass-based partitioning model to several other common predictive approaches. For each dry particle composition and size, cloud droplet activation is calculated from Eq. 1 by considering the influence of NAFA surface activity according to five different representations (summarized in Table 1):

- **(P)** The full partitioning model decribed in Section 2.1: For each droplet size, the NAFA bulk/surface partitioning equilibrium is solved iteratively from Eq. 6 to determine the droplet bulk phase composition $\{x_i^B\} = \mathbf{x^B}$, from which droplet surface tension and water activity are evaluated according to concentration-dependent ternary parametrizations, $\sigma = \sigma(\mathbf{x^B})$ and $a_\mathrm{w} = a_\mathrm{w}(\mathbf{x^B})$, according to Eqs. 8 and 11. By using measurement-based parametrizations which rely only on *mass* concentrations and mass mixing ratios of organic and inorganic components, a quantitative description is obtained with respect to all droplet components, including the chemically unresolved NAFA. This comprehensive thermodynamic formulation serves as a benchmark for the evaluation of effects of NAFA surface activity in cloud droplet activation, as well as for the performance of the other representations applied.

- **(S)** The simple partitioning model of Prisle et al. (2011): All surfactant solute is assumed to be completely partitioned to the droplet surface, such that $m_\mathrm{sft}^B = 0$ for all droplet sizes and compositions and the surface active particle components do not affect either water activity or surface tension at the point of activation. This representation is a simple empirical model based on the predictions of the thermodynamically consistent partitioning model of Prisle et al. (2010) for droplets comprising simple, strong, molecular surfactants (such as SDS) at the critical point of activation. Because the surface active components do not contribute to the composition-dependent droplet properties and the partitioning equilibrium does not need iteration, this representation is computationally simple and immediately applicable to chemically unresolved complex surface active mixtures. When all surfactant mass is depleted from the bulk, concentration-dependent droplet water activity is evaluated from the binary aqueous NaCl parametrization given by Prisle (2006) based on data from Low (1969):

$$a_\mathrm{w} = 1 - 0.031715 b_\mathrm{NaCl} + 0.0012582 b_\mathrm{NaCl}^2 - 0.000022921 b_\mathrm{NaCl}^3. \tag{12}$$

Here, b_NaCl is the molal concentration of NaCl, which is readily determined from the mass concentration *via* the well-known molar mass of NaCl. Droplet surface tension is constant $\sigma = \sigma_\mathrm{w}$.

(I) Insoluble surfactant model: Similar to (S), all surfactant solute is assumed to be completely partitioned to the droplet surface ($m_\mathrm{sft}^B = 0$), but the surface tension is reduced by a constant amount to either $\sigma = 0.95\sigma_\mathrm{w}$ or $0.80\sigma_\mathrm{w}$ throughout droplet growth. This corresponds to a simplified representation of an insoluble surfactant, where the surface active component does not dissolve into the bulk solution, but forms a phase-separated layer on the surface which reduces solution surface tension according to the surface coverage (Ruehl et al., 2016). Due to the lack of quantitative surface-composition based surface tension relations for chemically unresolved NAFA, the surface tension reduction is here represented with a constant value, similarly to the approach of Davies et al. (2019).

(B) Bulk solution model: The droplet is assumed to have the same properties as a macroscopic (bulk) solution of corresponding total composition. The surface partitioning factor is assumed to be negligible, such that the droplet bulk phase composition is determined directly from the total composition without iteration ($\mathbf{x^B} = \mathbf{x^T}$). Droplet surface tension and water activity are evaluated according to the same concentration-dependent mass-based ternary parametrizations (Eqs. 8 and 11) as for **(P)**. However, the bulk compositions at each droplet size will generally differ between the two representations.

(K) Basic Köhler model: Effects of surface activity are disregarded altogether. As for **(B)**, the droplet bulk phase composition is equal to the total droplet composition, without correction for surface partitioning ($\mathbf{x^B} = \mathbf{x^T}$). The surface tension is assumed to be constant for all droplet sizes and compositions and equal to that of pure water ($\sigma = \sigma_\mathrm{w}$). Droplet water activity is evaluated according to the concentration-dependent mass-based ternary parametrization in Eq. 11, using the total droplet composition $a_\mathrm{w} = a_\mathrm{w}(\mathbf{x^T})$.

Representations (P), (S), and (I) consider the impact of surface adsorption on bulk/surface partitioning of NAFA, whereas (B) and (K) are both bulk solution representations. Surface tension is reduced in (P) and (B) according to composition dependent relations, and by a constant value in (I). As the surface active component is completely partitioned to the surface in (S) and (I), only NaCl impacts water activity in these representations according to a binary relation, whereas a ternary water activity relation is used in (P), (B), and (K).

Strictly, only representation (P) requires the use of fully continuous ternary parametrizations, since only in these calculations does the relative NAFA–NaCl solute mixing ratio change from that of the dry particles ($w_i \neq W_{\mathrm{p},i}$) as the droplets grow. In representations (S) and (I), the relative bulk phase mixing state of NAFA and NaCl changes discontinuously at the onset of droplet growth, from the nominal dry particle value to $\{w_\mathrm{NAFA} = 0, w_\mathrm{NaCl} = 1\}$ in droplets where NAFA is completely partitioned to the surface. When representations (B) and (K) are used, the relative mixing ratio of NAFA and NaCl solutes

Table 1. Properties included in the different representations of NAFA surface activity used in Köhler calculations.

	representation	partitioning	$\sigma = \sigma_\mathrm{w}(\mathbf{x^B})$	$a_\mathrm{w} = a_\mathrm{w}(\mathbf{x^B})$
(P)	full partitioning	size- and composition-dependent, Eq. 6	Eq. 8	Eq. 11
(S)	simple partitioning	complete, $m^B_\mathrm{NAFA} = 0$	σ_w	Eq. 12
(I)	insoluble surfactant	complete, $m^B_\mathrm{NAFA} = 0$	$0.80\sigma_\mathrm{w}$, $0.95\sigma_\mathrm{w}$	Eq. 12
(B)	bulk solution	no, $\mathbf{x^B} = \mathbf{x^T}$	Eq. 8	Eq. 11
(K)	basic Köhler	no, $\mathbf{x^B} = \mathbf{x^T}$	σ_w	Eq. 11

remains equal to the nominal value of the dry particles and does not change with concentration of the growing droplets ($w_i = W_{\mathrm{p},i}$). For consistency, the ternary parametrizations given in Eqs. 8 and 11 are here used in all calculations, at essentially no additional computational cost. This allows us to compare features of the different surfactant representations also in terms of predicted droplet properties for continuous variation in dry particle compositions.

3 Results and discussion

In the following, we present results of modeled CCN activity and droplet properties during growth and at the critical point of activation for mixed NAFA–NaCl particles, using the different representations of NAFA surface active properties in aqueous solution droplets. By analyzing and comparing the results of each representation, the influence of various aspects of NAFA surface activity on predicted CCN activity is assessed. Model sensitivity to selected input parameters, including assumed NAFA mass density and average molar mass, droplet temperature, choice of surface tension equation, and the effect of potential sample impurity in the droplet activation measurements of Kristensen et al. (2014) is presented in Section S5 of the SI.

3.1 CCN activity

Modeled critical supersaturations (SS_c) as functions of dry particle diameter (D_p) are presented in Figure 1 for particles with dry NAFA mass fractions ($W_\mathrm{p,NAFA}$) of 0% (blue), 20%, (green), 50% (red), 80% (purple), and 100% (black), relative to NaCl. Results of Köhler calculations with each of the four representations of surfactant effects (P), (S), (B), and (K) are shown in panels a), b), c), and d), respectively, together with the experimental values for particles with equivalent dry compositions reported by Kristensen et al. (2014) for comparison. Error bars on the experimental data are estimated as ± 1 standard deviations on measured SS_c, as reported by Kristensen et al. (2014). Model results for representation (I) are shown in Section S1 of the SI.

All representations of NAFA surface activity give similar results in the limit of pure NaCl particles, as expected. For each representation, the modeled CCN activity decreases (SS_c increases) with increasing $W_\mathrm{p,NAFA}$ for a given particle size, in agreement with the experimental trend. This shows that upon varying the dry particle composition from pure NaCl to pure NAFA, any effect of decreased droplet surface tension at the point of activation, from the presence of surface active NAFA in the droplet phase, cannot overcome the simultaneous increase in water activity (Eq. 2), arising from a potential combination

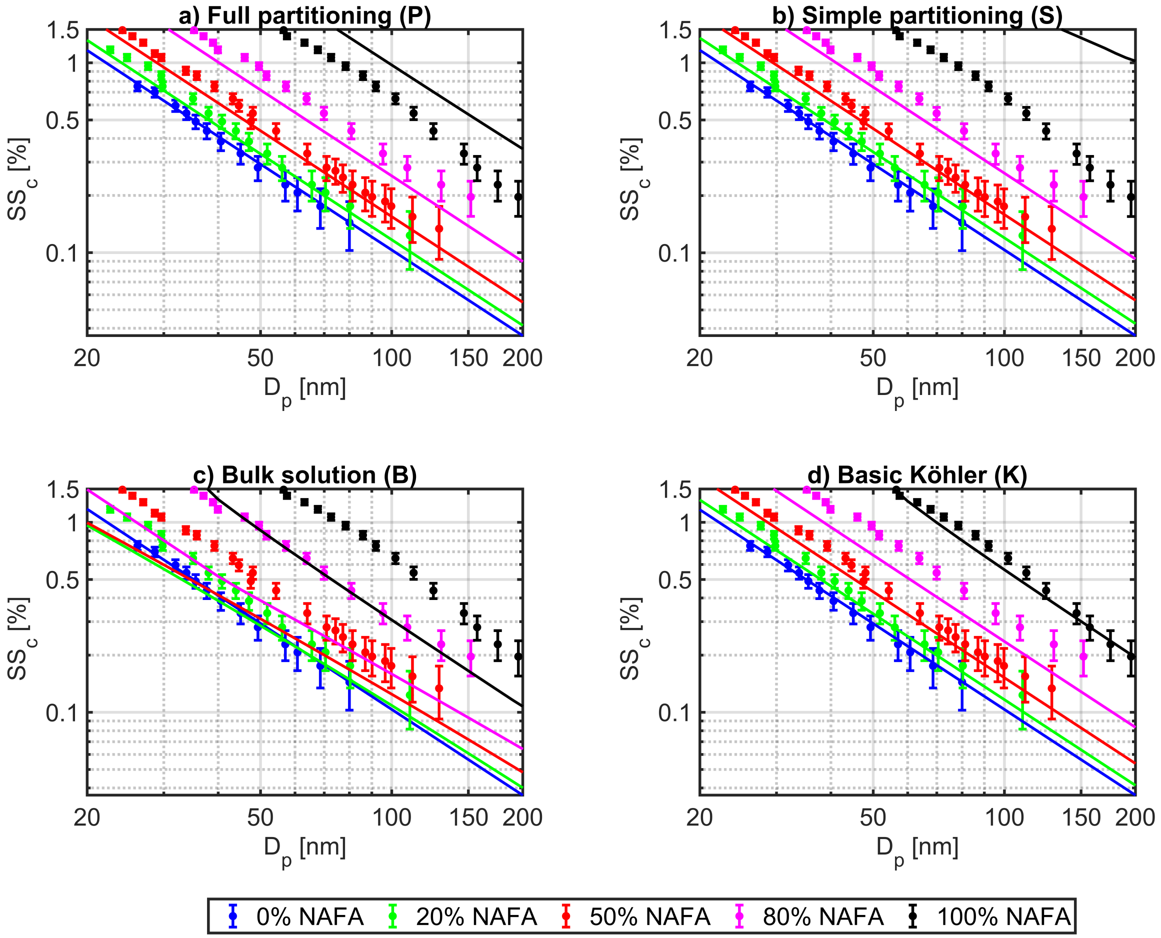

Figure 1. Critical supersaturations (SS_c) for mixed NAFA–NaCl particles, calculated (curves) using the different representations of NAFA surface activity described in Section 2.3: (a) full partitioning model (P), (b) simple partitioning model (S), (c) bulk solution model (B), and (d) basic Köhler model (K), in each case compared to experimental values (dots) measured by Kristensen et al. (2014). Colors indicate the original dry particle fraction of NAFA ($W_\mathrm{p,NAFA}$) relative to NaCl. Calculations are made using a NAFA mass density of $\rho_\mathrm{NAFA} = 1.6\ \mathrm{g\ cm^{-3}}$. Error bars on experimental data represent ± 1 standard deviations on SS_c as reported by Kristensen et al. (2014).

of *i*) increasing droplet non-ideality (specifically leading to increased $\gamma_\mathrm{w} > 1$), *ii*) depletion of solute from the droplet bulk phase due to NAFA surface partitioning, and *iii*) the much higher average molar mass of NAFA, compared to pure NaCl (both leading to increased x_w^B). Several studies have previously observed the same trend, experimentally or in model calculations, for aerosol systems comprising both simple strongly surface active molecules, such as SDS and fatty acid sodium salts (Li et al., 1998; Sorjamaa et al., 2004; Prisle et al., 2008, 2010; Petters and Petters, 2016; Forestieri et al., 2018), as well as complex macromolecules and surface active mixtures (Hansen et al., 2015; Dawson et al., 2016; Prisle et al., 2019), in various mixing ratios with NaCl.

The overall good performance of calculations using (P) with respect to measured CCN activity is reassuring in terms of our ability to capture relevant properties of the activating droplets within the comprehensive thermodynamic description. Each of the representations (P), (S), and (K) describe the experimental data fairly well, except in the case of pure NAFA particles, where (P) and (S) underestimate CCN activity well outside the reported experimental uncertainty. In the absence of hygroscopic NaCl, predictions with model (S) correspond to condensation of water into a pure aqueous droplet phase in the presence of insoluble material, which is adsorbed at the droplet surface without attaining full coverage. Similarly for the insoluble surfactant model (I), shown in Fig. S3 in the SI, but here the reduced surface tension brings predictions somewhat closer to experimental values for pure NAFA particles, compared to (S). To reconcile predictions of model (I) with measured SS_c for pure NAFA particles would however require much stronger surface tension reductions than the 5–20% included in the present calculations, at the expense of increasingly poor agreement with experimental values for all other particle compositions. In general, it is clear that model (I) does not represent experimental CCN data well across the full range of NAFA–NaCl particle sizes and compositions investigated. This suggests that discrepancies observed for the other partitioning models (P) and (S) for particles with the highest mass fractions of NAFA cannot be attributed to surface tension effects alone. It is possible that relatively small amounts of hygroscopic impurities could be present in the NAFA aerosol mixture and thus enhancing experimental CCN activity, as first described by Bilde and Svenningsson (2004). The model sensitivity analysis presented in Section S4 of the SI shows that even 3% by mass of impurities in the NAFA mixture with hygroscopic properties corresponding to those of NaCl would be sufficient to reconcile the calculations of model (P) with experimental data for pure NAFA particles. For the simple partitioning model (S), 5% by mass of such impurities could similarly reproduce the measured CCN activity, whereas the agreement with experiments for both bulk solution models (K) and (B) decreases when assuming impurities in the NAFA mixture.

A prominent feature of Fig. 1 is how Köhler calculations using the bulk solution representation (B) clearly and consistently underestimate experimental critical supersaturations for all particle sizes and compositions. Similar observations have been made in several previous studies at both sub- and supersaturated conditions, for particles comprising both chemically simple and complex surfactants, and for both pure surfactant particles and in various mixtures with inorganic salts (Li et al., 1998; Rood and Williams, 2001; Sorjamaa et al., 2004; Prisle et al., 2008, 2010; Harmon et al., 2010; Ruehl et al., 2010; Zamora and Jacobson, 2013; Kristensen et al., 2014; Hansen et al., 2015; Petters and Petters, 2016; Forestieri et al., 2018; Prisle et al., 2019). Our present results confirm that bulk/surface partitioning of strongly surface active aerosol components must be taken duly into account if the impact on droplet surface tension is considered in predictions of CCN activity. Model (K) tends to overestimate mixed NAFA–NaCl experimental CCN activity slightly more than the partitioning models (P) and (S), further suggesting that NAFA bulk depletion from surface partitioning may indeed have a more significant impact on decreasing CCN activity than surface tension reduction has on increasing it.

Kristensen et al. (2014) originally compared their measured CCN activities to two simple bulk solution Köhler models based on similar assumptions as representations (B) and (K) of the present work, with some differences in the actual model implementation. In this work, models (B) and (K) are for consistency run with the continuous ternary surface tension and water activity parametrizations presented in Eqs. 8 and 11, even if these are not strictly needed in absence of bulk/surface partitioning calculations. Kristensen et al. (2014) used simpler parametrizations with a 1-dimensional composition domain, which are not continuous with respect to variations in the relative NAFA–NaCl mass fractions in solution w_{NAFA} and w_{NaCl} and have slightly different functional forms than the full ternary functions used here, even at the lines of intersection. Furthermore, the surface tension parametrizations used by Kristensen et al. (2014) are made for data points corresponding to measurement times t$=0$ s after the formation of the surface and therefore based on higher surface tension values for a given solution composition, compared to the data from measurement times t$=600$ s used in this work. As higher macroscopic surface tensions correspond to lower surface activity of NAFA, their predictions of SS_{c} using a bulk solution model are similarly biased higher, partially mimicking the elevated surface tension in droplets due to surface partitioning. However, as clearly seen from Fig. 7 of Kristensen et al. (2014), this effect still is not sufficient bring Köhler predictions even close to agreement with their CCN experiments.

Similar to the present model (K), Kristensen et al. (2014) also find that a basic Köhler model, where NAFA surface activity is completely ignored, gives good agreement with measured CCN activity for NAFA–NaCl particles with up to 50% NAFA, as well as for pure NAFA, but not for particle mixtures with 80% NAFA. This seemingly counter-intuitive result for particle mixtures comprising strongly surface active material with significant ability to lower surface tension in macroscopic solutions has been observed also for simple, strong surfactants, such as SDS and C8-C12 fatty acid salts (Sorjamaa et al., 2004; Prisle et al., 2008, 2010, 2011). On the other hand, several recent studies have shown properties for both simple and complex aerosol mixtures, including secondary organic aerosol (George et al., 2009; Ruehl et al., 2016), limonene-derived organosulfate products (Hansen et al., 2015), marine primary organics (Ovadnevaite et al., 2017), and water-soluble pollen extracts (Prisle et al., 2019) which are consistent with an enhancement of aerosol hygroscopicity by surfactants, at least partly due to reduced surface tension. This suggests that model (K) is too simple to fully capture CCN activity of different types of surface active aerosol components and in all mixing states and that, generally, a full partitioning model is needed for robust predictions. In cases where the basic Köhler model (K) gives good agreement with experimental CCN activity, it also closely traces predictions with the comprehensive partitioning model (P).

3.2 Droplet properties at activation

Figure 2 (a) presents critical supersaturations as a function of NAFA mass fraction $W_{\mathrm{p,NAFA}}$ in the dry particles calculated with each model representation for 50 nm dry particles. Experimental values from Kristensen et al. (2014) for particles with similar dry sizes are shown for reference: immediate comparison is not always possible along the particle composition dimension, because Kristensen et al. (2014) used an experimental setup scanning a set of pre-selected supersaturations, rather than particle sizes, and therefore did not measure the exact same particle sizes for each dry particle composition. Corresponding to each value of SS_{c} shown in panel (a), the other panels in Fig. 2 show for the same 50 nm particles, also calculated at the critical point d_{c} of the Köhler curve: (b) the individual Kelvin and Raoult terms, (c) droplet diameter growth factor $GF_{\mathrm{c}}=d_{\mathrm{c}}/D_{\mathrm{p}}$, and (d) droplet surface tension σ_{c}. Qualitatively similar results were obtained for other dry particle sizes, but differences between

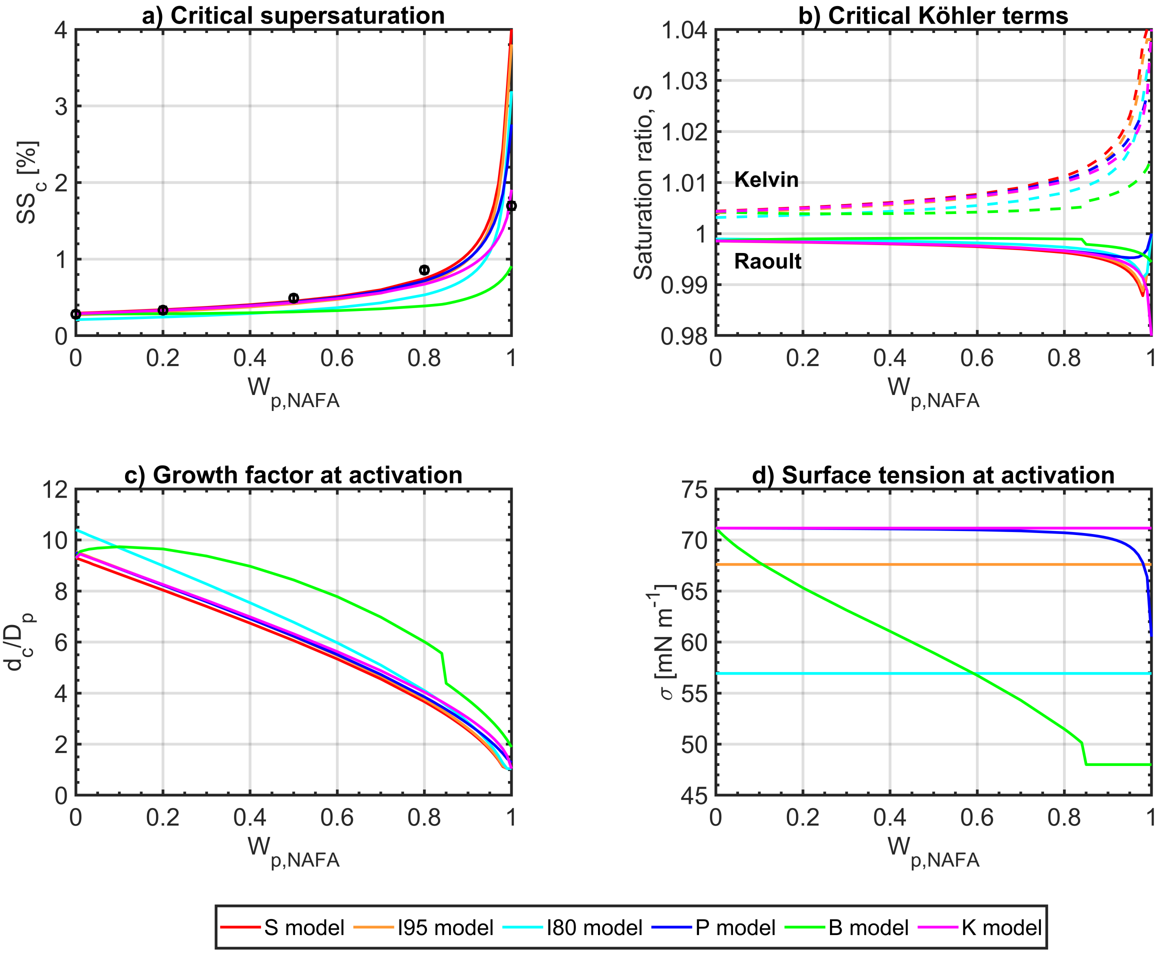

Figure 2. Properties of activating droplets calculated with representations (P), (S), (I), (B) and (K) at the critical point of droplet activation d_c for 50 nm dry particles as functions of dry particle NAFA mass fraction $W_\mathrm{p,NAFA}$: (a) critical supersaturations SS_c, (b) Kelvin and Raoult terms at the critical point of the Köhler curve corresponding to each SS_c, (c) droplet diameter growth factor, and (d) droplet surface tension. In panel (a), experimental values from Kristensen et al. (2014) for particles with similar dry sizes are shown for reference.

model are more pronounced for smaller particles, which generally activate for smaller critical sizes, corresponding to smaller critical growth factors, with more concentrated droplet compositions and larger surface area-to-bulk volume ratios, introducing more pronounced effects of surface partitioning for a given total composition.

Results in Fig. 2 (a) illustrate how the full partitioning model (P) trace experimental CCN activity well, but also highlights the strong sensitivity of model predictions to NAFA mass fraction in the particles at the highest $W_\mathrm{p,NAFA}$. As discussed in detail below, this sensitivity is due to predicted droplet states with highly depleted bulk phases, for which the partitioning of a single mass unit of surface active solute leads to large changes in bulk (and surface) mass concentrations of the finite-sized droplets. A similar phenomenon was noted by Malila and Prisle (2018) and is further exaggerated for the present particle compositions by the very large average molar mass of the NAFA mixture.

Fig. 2 (a) shows that the simple representations (S) and (I), as well as the basic Köhler model (K) all predict very similar properties of activating droplets to those of the full partitioning model (P) for essentially the entire range of NAFA mass fractions in the particles. A similar close agreement between basic Köhler predictions and comprehensive partitioning thermodynamics has also been observed in previous studies for particles comprising simple strong surfactant–salts mixtures (Prisle et al., 2010, 2011; Forestieri et al., 2018). For NAFA particles, the agreement between models here extends to even larger surfactant fractions (up to about 80% by mass of NAFA) than seen in the earlier studies. Furthermore, not only critical supersaturations, but also the individual Kelvin and Raoult terms at the point of droplet activation in Fig. 2 (b) and predicted droplet sizes at activation as represented by the droplet growth factors in Fig. 2 (c) also agree well between these models. This was not immediately expected, since model (S) was proposed to emulate specifically SS_c, not necessarily other droplet properties at the critical point (Prisle et al., 2011), and since NAFA is seen from experimental data to give significant surface tension reductions in macroscopic solutions (Kristensen et al., 2014), contrary to the assumptions of both models (S) and (K). Fig. 2 (d) shows that the full partitioning model (P) predicts surface tensions of activating droplets which are very close to that of pure water, and for nearly the entire dry particle composition range is within the range of constant values assumed in models (S), (I) and (K). The similarity of all activation parameters indicates that the underlying assumptions of both the simple representations and the basic Köhler model are reasonably representative for the NAFA particle systems in question, as predicted by the comprehensive model (P).

It is important to note that properties in Fig. 2 correspond to critical droplets of different sizes d_c. Variations of critical droplet properties with $W_\mathrm{p,NAFA}$ represent only the maxima of individual Köhler curves corresponding to each particle composition and therefore do not *a priori* reflect continuous variation in all underlying droplet properties. In addition to the overall variation in total solute composition given by $W_\mathrm{p,NAFA}$, also the droplet dilution state, as seen by the varying activation growth factors GF_c (panel c), and the ensuing size-dependent bulk/surface partitioning of NAFA predicted with representation (P) according to the changing A/V and dilution state vary between the critical droplets. Total composition, dilution, and partitioning each affect the droplet bulk solution composition, from which the droplet surface tension (panel d) and Kelvin and Raoult terms (panel b) are evaluated.

3.2.1 Raoult effects

The Raoult terms shown in Fig. 2 (b) each vary as functions of $W_\mathrm{p,NAFA}$, when the mass of hygroscopic NaCl is gradually replaced with the significantly less hygroscopic component NAFA, and in response to the changing critical droplet dilution state, affecting both the overall amount of water and solute in the droplets, and in the case of representations (P), (S), and (I) also the extent of NAFA bulk/surface partitioning. Each of these mechanisms affect the composition of the droplet bulk phase, which govern a_w according to Eq. 2 in general and Eqs. 11 or 12 for the present calculations in particular. The calculated critical Raoult terms are seen to be *higher* for the bulk solution representation (B) than the other representations, despite that

(P), (S) and (I) consider bulk depletion of NAFA, whereas (B), like (K), does not. This is due to the significantly higher dilution factor of activating droplets predicted by (B), as is seen from GF_c in Fig. 2 (c). For representations (P), (S) and (I), both the predicted Raoult terms and growth factors of activating droplets are mutually very similar. For all representations, the predicted reduction of water activity at droplet activation is modest across the full dry particle composition range, reflecting the overall dilute critical droplet state and the modest impact of NAFA on particle hygroscopicity.

For the partitioning representations (P), (S), and (I), an inflection point is seen in the Raoult terms for very high $W_\mathrm{p,NAFA}$, whereas for the bulk solution representations (B) and (K), the Raoult terms decrease with increasing $W_\mathrm{p,NAFA}$ throughout the dry particle composition range. In the absence of bulk/surface partitioning, droplet concentrations continue to increase with decreasing dilution of the total solute mass, as seen from the growth factors GF_c in Fig. 2 (c). When bulk/surface partitioning of NAFA is considered, the effect of decreasing dilution is first strong enough to overcome the decrease in total amount of hygroscopic material with increasing $W_\mathrm{p,NAFA}$ and the depletion of NAFA from the droplet bulk, leading to decreasing Raoult terms, but eventually the balance reverses, as the total amount of NaCl in the droplets becomes too small to compensate for the surface active component which is largely depleted from the bulk. With the full partitioning model, the Raoult term of the critical droplets changes smoothly with $W_\mathrm{p,NAFA}$, whereas sharp inflection points are seen for the simple models (S) and (I), where partitioning is described as a step function.

The predicted bulk compositions of activating droplets are presented in Fig. S2 and discussed in detail in Section S2 of the SI. The NAFA surface partitioning factor at droplet activation, in terms of the mass ratio of NAFA solute in the droplet surface and bulk, $m^S_\mathrm{NAFA}/m^B_\mathrm{NAFA}$, calculated with the full partitioning representation (P), is shown in Fig. S2 (c). In representations (S) and (I) with complete surface partitioning, this value is infinite at all droplet sizes, and in the bulk solution models (B) and (K), it is 0. Fig. S2 (d) shows the resulting droplet bulk composition in terms of the mass fraction of solute comprised by NAFA, $w_\mathrm{NAFA} = m^B_\mathrm{NAFA}/(m^B_\mathrm{NAFA}+m^B_\mathrm{NaCl})$, at the point of droplet activation. For calculations with (B) and (K), this ratio is identical to the dry particle composition $W_\mathrm{p,NAFA}$, as it should be in the absence of bulk depletion from surface partitioning of NAFA. With representations (S) and (I), the NAFA bulk solute fraction is vanishing, since $C_\mathrm{NAFA} = 0\ \mathrm{g\ L^{-1}}$. Partitioning of NAFA profoundly changes the droplet bulk phase mixing state at the point of activation, compared to the relative NAFA–NaCl ratio in the original dry particles. For 50 nm particles, $m^S_\mathrm{NAFA}/m^B_\mathrm{NAFA}$ in activating droplets calculated from the comprehensive partitioning model (P) is larger than 500 for all particle compositions and for all dry particle sizes and NAFA mass fractions investigated (Fig. 1), calculated $m^S_\mathrm{NAFA}/m^B_\mathrm{NAFA}$ at the point of activation is greater than two orders of magnitude (not shown). As a result, except for the very largest dry particle NAFA fractions, the concentration of NAFA (Fig. S2a) and the relative amount of droplet solute comprised by NAFA (Fig. S2d) in activating droplets is all but vanishing. These observations support the applicability of the underlying assumptions in the simple representation (S) for NAFA CCN activity, that the surfactant bulk concentration at droplet activation is effectively 0 and the overall impact of NAFA on particle hygroscopicity is vanishing.

For representation (B), the predicted Raoult term of critical droplets has a step change with respect to the dry particle composition at $W_\mathrm{p,NAFA} = 0.85$. The corresponding increasing concentrations of both NAFA and NaCl are clearly seen in Figs. S2 (a) and S2 (b) in the SI. This is caused by a predicted step decrease in the critical droplet growth factors GF_c (Fig. 2c), leading to a simultaneous step increase in the Kelvin term (Fig. 2b). As seen in Fig. 2a, the opposing changes in the Kelvin and Raoult terms caused by decreasing d_c cancel out, so that the resulting SS_c predicted with model (B) change smoothly with $W_\mathrm{p,NAFA}$. At the same dry particle composition, critical droplet surface tensions σ_c in Fig. 2 (d) predicted with representation (B) reach a constant minimum value. This corresponds to droplets exceeding a critical micelle concentration-type transition for NAFA, which is estimated from the surface tension data of Kristensen et al. (2014) to occur for various NAFA–NaCl mixtures at $\sigma = 48\ \mathrm{mN\ m^{-1}}$. Figures 3 and 4 (discussed in more detail below) show how the critical point d_c predicted with model (B) shifts between two local maxima on the Köhler curve, from the larger to the smaller droplet size, corresponding to droplets with surface tensions above, or at, the minimum value, respectively. This causes the discontinuous shift in d_c and other critical droplet properties seen for representation (B) in Figs. 2 and S2. A similar shift is not seen for calculations with representation (P), because the droplet surface tension never reaches the minimum value $\sigma = 48\mathrm{mN\ m^{-1}}$ (Figs. 2d and 4).

3.2.2 Kelvin effects

The Kelvin term at droplet activation depends on the critical droplet size d_c, determining the curvature effect according to Eq. 1, together with the droplet surface tension as a function of droplet bulk composition, which in turn is governed by the droplet dilution state and size-dependent bulk/surface partitioning. The critical Kelvin terms for each NAFA representation in Fig. 2 (b) generally follow the corresponding trends in d_c as given by GF_c (Fig. 2c). Figure 2d shows how droplet surface tension at activation is reduced according to Eq. 8 in calculations with (P) and (B), or fixed to σ_w, $\sigma = 0.95\,\sigma_\mathrm{w} \approx 68\ \mathrm{mN\ m^{-1}}$, and $\sigma = 0.80\,\sigma_\mathrm{w} \approx 57\ \mathrm{mN\ m^{-1}}$ for models (K), (I95), and (I80), respectively. When the critical surface tension is significantly reduced in calculations with (B) and (I80), the corresponding Kelvin terms are somewhat lower than for (P), (S), and (I95), where surface tension is only modestly reduced at activation, or not at all.

Predictions with representation (B) in Fig. 2 (d) show how, despite higher predicted dilution states, NAFA can significantly reduce surface tension of activating droplets when they are considered similar to macroscopic solutions, whereas for representation (P) the predicted surface tensions at droplet activation are overall only modestly reduced. For particles comprising less than 80% by mass of NAFA, the surface tensions in activating droplets are essentially the same as for pure water and only for the very highest mass fractions of NAFA ($W_\mathrm{p,NAFA} > 0.95$) is the surface tension reduced by more than 5% from the pure water value. This is one of the fundamental assumptions underlying calculations with both (S) and (K) – and the validity of this assumption as predicted with (P) for all but the largest dry particle NAFA fractions is one of the main drivers of the simultaneous close agreement between predictions with (S) and (K), and the comprehensive framework of (P). Furthermore, the effect of any modest surface tension reduction at the point of droplet activation must be more than counterbalanced by bulk depletion from NAFA surface partitioning, since the predicted SS_c are higher for (P) than for (K), but slightly higher in (S) than for (P), at the highest NAFA fractions. This is also reflected in the corresponding Raoult terms.

3.3 Properties of growing droplets along Köhler curves

Figure 3 shows the Köhler curves for selected dry particle compositions $W_\mathrm{p,NAFA} =$ (a) 0.20, (b) 0.50, (c) 0.80, and (d) 0.95, calculated with each model representation for the 50 nm particles described in Figs. 2 and S2.The droplet surface tensions evaluated along the Köhler curves are shown in Fig. 4 and the corresponding NAFA surface partitioning factors

$m^S_{\mathrm{NAFA}}/m^B_{\mathrm{NAFA}}$ and water activities of the growing droplets are presented in Figs. S4 and S5 of the SI. All representations used in calculations of CCN activity produce meaningful Köhler curves and other solution properties for the growing droplets. For all curves representing calculated properties of the growing droplets, the respective critical points of droplet activation calculated with each model (SS_{c} presented in Figs. 1 and S1) are indicated with asterisks.

The close agreement between partitioning representations (P), (S), (I95) and the basic Köhler model (K) for calculated droplets properties at the point of activation d_{c} is evident along the full Köhler curves in Fig. 3, except for the highest NAFA fraction in the dry particles $W_{\mathrm{p,NAFA}} = 0.95$ (panel d). Here, clear differences in the shapes of the calculated Köhler curves can be seen, as the representations of NAFA surface activity become more prominent relative to the still smaller amount of hygroscopic NaCl in the droplets. For both representations (B) and (I80), the predicted droplet surface tension in Fig. 4 is significantly reduced during droplet growth and well beyond the point of activation. At a given droplet size d, the equilibrium supersaturation SS is higher for representation (B) than for (I80) when the concentration-dependent droplet surface tension is higher in (B) than the fixed surface tension of $\sigma = 0.80\sigma_{\mathrm{w}}$ in (I80), and vice versa. For representations (P), (S), and (I95), the order of the Köhler curves, as well as the values of SS_{c} at the critical points, do not simply follow the relative magnitudes of the droplet surface tensions at each d. In calculations with the full partitioning model (P), surface tension is reduced for the more concentrated droplets at the earlier stages of the Köhler growth curves, but only for the highest $W_{\mathrm{p,NAFA}} = 0.95$ in Fig. 4 (d) is the reduction maintained until the critical point. Even for droplets much smaller and more concentrated than at the point of activation ($d < d_{\mathrm{c}}$), surface tension is never reduced by more than about 10% from the pure water value. This reflects the very small amounts of NAFA solute remaining in the finite-sized droplet bulk phase, when bulk/surface partitioning is taken into consideration.

The degree of NAFA partitioning to the surface is significant already at the much higher total droplet concentrations at the early stages of the Köhler curves before activation and generally the amount of NAFA in the droplet surface is 2-3 orders of magnitude higher than the amount left in the bulk (Fig. S4). Typically, $m^S_{\mathrm{NAFA}}/m^B_{\mathrm{NAFA}}$ is even higher for droplet sizes $d < d_{\mathrm{c}}$ than at the critical point, illustrating that partitioning has an even greater effect on the droplet bulk concentration of NAFA than the lower degrees of dilution in the smaller droplets. As a consequence, even if NAFA is able to significantly reduce surface tension in macroscopic solutions, the same impact is not seen in microscopic activating droplets, even at corresponding total droplet concentrations. The differences between surface tension variations predicted with Eq. 8 in macroscopic and microscopic droplet solutions due to changes in bulk composition from NAFA partitioning are further discussed in Section S4 of the SI.

Fig. S4 shows how the water activity increases as droplets grow and dilute along the Köhler curves. Predicted droplet a_{w} only differ significantly between the different representations when NAFA fractions in the dry particles are very large. The water activity is significantly reduced early in droplet growth, but except for the largest $W_{\mathrm{p,NAFA}}$ is very close to 1 when droplets reach d_{c}. As NAFA is much less hygroscopic than NaCl, and the resulting reduction of water activity is even smaller for sub-micron droplets due to strong bulk/surface partitioning, a_{w} predicted with model (P) is governed by the hygroscopic salt variations along the Köhler curve mainly reflect the changing droplet dilution state.

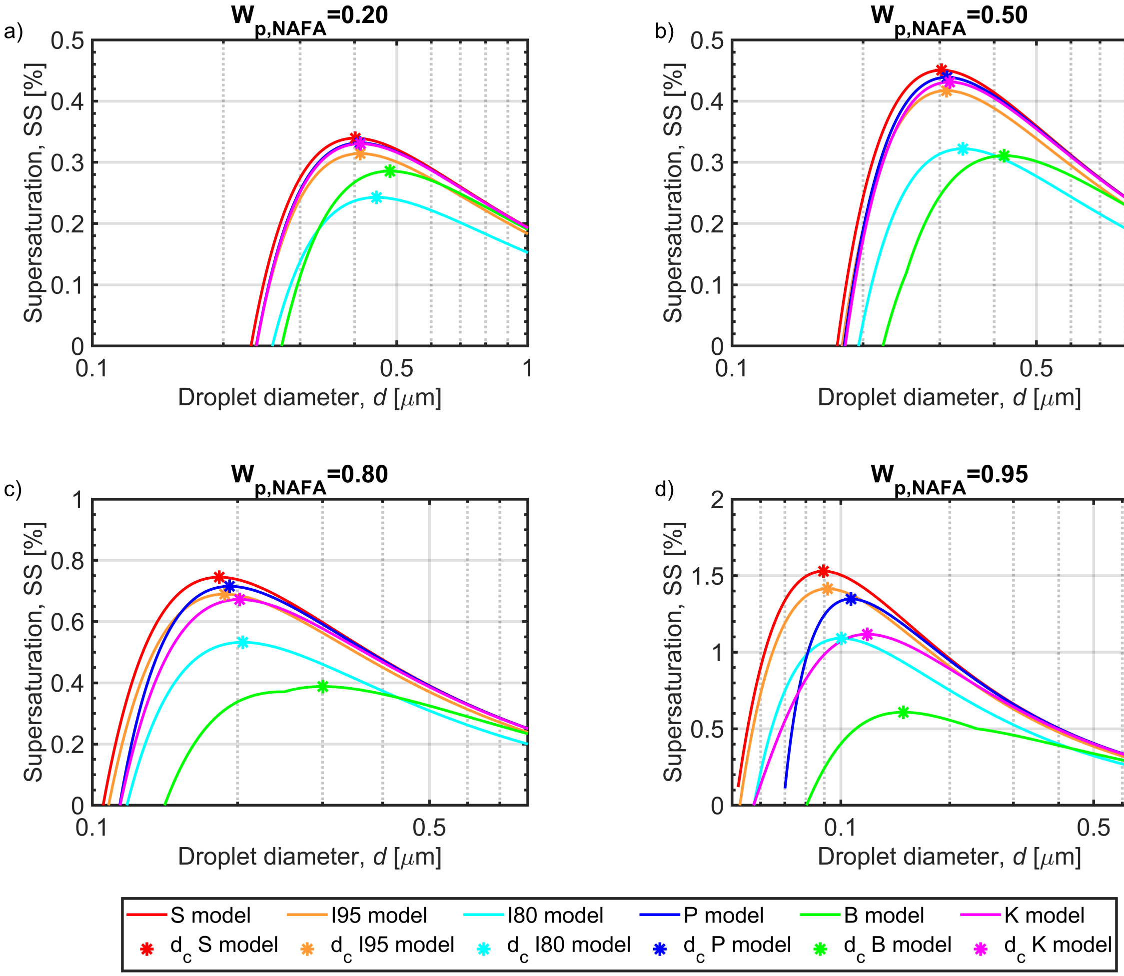

Figure 3. Köhler curves for growing aqueous NAFA–NaCl droplets formed from 50 nm dry particles with NAFA mass fractions of (a) 0.20, (b) 0.50, (c) 0.80, and (d) 0.95, calculated with the different models described in Section 2.3. The critical points of droplet activation (SS_c) presented in Figs. 1 and S3 are indicated with asterisks on each Köhler curve. Note that the supersaturation (SS) scale is different between the panels.

3.4 Implications for Köhler modeling

In the following section, we summarize the main insights from the comprehensive Köhler modeling of droplet growth and activation dynamics for complex surface active aerosol mixtures and the comparison of the full mass-based partitioning model to the simpler predictive representations. We briefly contrast our mass-based Gibbisan model to other approaches to evaluating bulk/surface partitioning and surface tension in activating droplets. Based on our findings, we discuss some of the implications

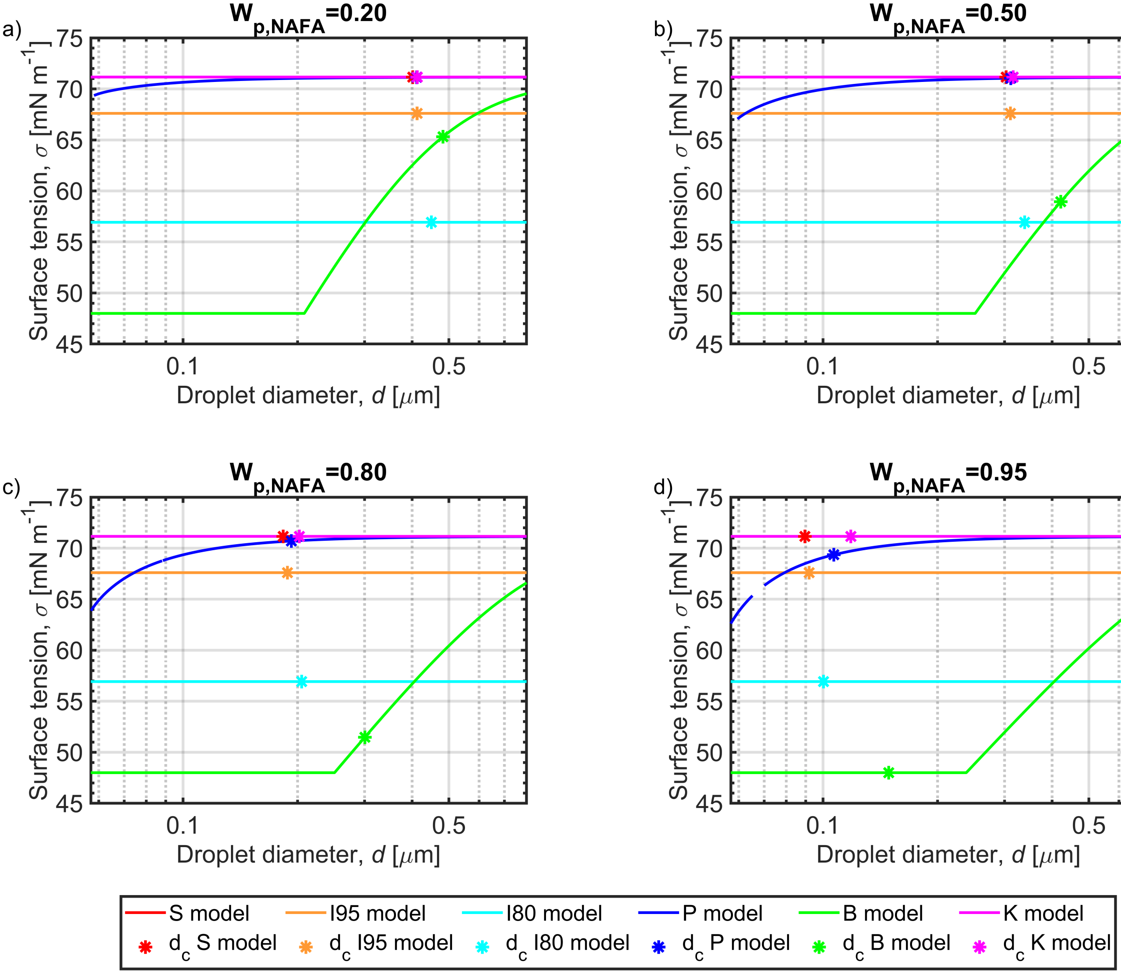

Figure 4. Surface tension along Köhler curves for growing aqueous NAFA–NaCl droplets formed from 50 nm dry particles with NAFA mass fractions of (a) 0.20, (b) 0.50, (c) 0.80, and (d) 0.95, calculated with the different models described in Section 2.3. The critical points of droplet activation (SS_c) presented in Figs. 1 and S3 are indicated with asterisks on each surface tension curve.

for understanding and modeling cloud microphysics of complex surface active aerosol in the atmosphere and for the prospect to include such process-level mechanisms in large scale atmospheric model applications.

3.4.1 Representation of strongly surface active aerosols

In this work, we find that cloud droplet growth and activation behavior of complex NAFA mixtures is driven by very similar mechanisms as has been found in earlier works for simple, strong surfactants. The comprehensive thermodynamic partitioning model (P) consistently during droplet growth and at the point of activation predicts the vast majority of NAFA in the droplet to be depleted from the bulk by partitioning to the surface. Except for particles with the very highest dry mass fractions, NAFA contributes next to none of the solute in the droplet bulk phase, which governs the equilibrium surface tension and water activity of the droplet. Even if NAFA effectively reduces surface tension in macroscopic solution, at droplet activation, the predicted surface tension is barely reduced at all for particles with less than 80% NAFA and for still higher NAFA fractions, the maximum surface tension reduction only amounts to around $10\ \mathrm{mN\ m^{-1}}$ from the pure water value across the investigated dry particle size range.

The basis for this seemingly counter-intuitive droplet state is the comparatively very large surface areas (A) relative to the finite volume (V) of the bulk for microscopic activating cloud droplets, compared to a macroscopic solution (Prisle et al., 2010; Bzdek et al., 2020). Even when essentially all the surface active material is adsorbed at the droplet surface, the finite-sized solution droplets do not comprise enough surface active solute altogether to generate sufficient surface (or bulk) concentrations to significantly reduce droplet surface tension. The equilibrium bulk-to-surface concentration gradient governing the adsorption of a surface active substance is therefore established for a droplet solution state of dilute concentrations in both bulk and surface phases. The pronounced bulk phase depletion further diminishes the low intrinsic hygroscopicity of the NAFA mixture, as seen in terms of impact on bulk water activity, to yield a nearly vanishing effective hygroscopicity in activating droplets. This leads to the strongly surface active component effectively behaving in small droplets as an insoluble and only slightly or even non-surface active substance.

These mechanisms explain the observed good performance of the simple partitioning model (S), where contributions from NAFA to both water activity and surface tension reduction are effectively set to zero, with respect to both experimental data and the comprehensive partitioning model (P). Similarly to previous results for the simple, strong surfactants SDS and fatty acid salts (Prisle et al., 2011), we here see that conditions for a range of droplet sizes, including at the critical point of activation, are closely represented by the simple partitioning model (S) also in the case of strongly surface active complex NAFA particles, as benchmarked by the comprehensive thermodynamic model (P). This establishes the simple partitioning model as a promising representation for other complex and unresolved surface active aerosol mixtures relevant to the atmosphere.

In a macroscopic solution, a strong surfactant which is fully partitioned to the surface would be expected to significantly reduce solution surface tension and the situation described by model (S) is of course quite unrealistic. However, the very poor performance of model (B) with respect to both CCN data from Kristensen et al. (2014) and predictions of the thermodynamic partitioning model (P), in contrast to the good performance of (S), shows that for the studied NAFA–NaCl mixtures, the most significant impact of surface activity on cloud microphysics is on bulk-phase depletion from surface partitioning, and notably *not* on surface tension reduction in activating droplets. Calculations with model (P) use the same composition-dependent surface tension and water activity relations as model (B), based on measurements made for macroscopic solutions (Eqs. 8 and 11). Several previous studies have highlighted that application of macroscopic relations without correcting the droplet bulk composition for depletion of surface active components from bulk/surface partitioning onto the large droplet surfaces fails to reproduce experimentally observed CCN activity for a variety of surface active organic aerosol (Li et al., 1998; Prisle et al., 2008, 2010, 2011; Petters and Petters, 2016; Forestieri et al., 2018; Lin et al., 2018). When macroscopic composition-dependent relations for surface tension, as well as other solution properties, are connected to microscopic droplet states *via* a bulk/surface partitioning model, the effect of bulk/surface partitioning in droplets is to move the solution mixing state to a different point in the composition domain, as illustrated in Figs. 2 and S2 for the present case of NAFA–NaCl droplet mixtures.

Similarly to several previous studies for particle mixtures of strong, simple surfactants SDS and fatty acid salts with NaCl, we also see that including surface tension effects of surface active NAFA aerosol without considering the altered bulk-phase composition from surface partitioning will lead to greater errors in estimating CCN activity than neglecting surface activity altogether (Sorjamaa et al., 2004; Prisle et al., 2008, 2010; Forestieri et al., 2018). As in the previous studies, detailed comparison to predictions with the comprehensive partitioning model (P) showed that the good agreement of the basic Köhler model (K) with measured CCN activity and close resemblance to model (P) are in large part due to cancellation effects between the perturbations in predicted Kelvin (surface tension depression) and Raoult (water activity depression) terms of the Köhler curves introduced by a full account of surface activity, compared to the basic Köhler model. This nearly full cancellation of surface activity effects on Kelvin and Raoult terms may not be present in droplet activation for all types of surface active aerosol components and mixtures, but could rather prove to be a signature feature of CCN activity for relatively strong surfactants.

3.4.2 Favorable conditions for reduced droplet surface tension

Several recent studies have presented results which are consistent with an enhancement of effective aerosol hygroscopic properties by surfactants, at least partly due to reduced surface tension, even when bulk/partitioning has been accounted for. Ovadnevaite et al. (2017) modeled nascent ultrafine mode (NUM) particles, with diameters up to 50 nm and comprising approximately equal contributions of organics and non-sea-salt sulphate, measured in North Atlantic marine air masses at Mace Head, using organic proxy mixtures comprising well-known secondary organic aerosol components and diarboxylic acids. They showed that while surface tension and bulk depletion effects may cancel for the larger particles, surface tension lowering can for the NUM particles prevail over the reduction in the Raoult effect and lead to substantial increases in CCN activity. Ruehl et al. (2016) measured the sizes of activating droplets along the Köhler curves and at the point of CCN activation for ammonium sulfate particles coated by dicarboxylic acids or α-pinene ozonolysis secondary organic aerosol and found that the shape of the growth curves and resulting critical droplet sizes were best described by accounting for both surface partitioning and reduced droplet surface tension. By comparing measurements of CCN activity for surface active limonene-derived organosulfate products (SOA compounds) and water-soluble pollen extracts (POA compounds) in mixtures with ammonium sulfate to predictions with a similar set of models as used in this work, Hansen et al. (2015) and Prisle et al. (2019) showed that experimentally determined droplet activation was consistent with presence of both moderate bulk-phase depletion and reduced droplet surface tension. George et al. (2009) found evidence for enhancement of CCN activity from reduced surface tension by surface active oxidation products in complex aerosol mixtures formed by chemical ageing of submicron Bis-2-ethylhexyl sebacate (BES) and stearic acid particles in a reactor flow tube.

Similar mechanisms could also be present for the bacterial biopolymers investigated by Dawson et al. (2016) as proxy for complex marine hydrogels. These substances produce significant surface tension reduction in macroscopic solutions (Lee et al., 2012), which is not reflected in experimental hygroscopic properties for aerosol mixtures with various salts. Dawson et al. (2016) suggested crosslinking between polymers and formation of insoluble complexes as a possible explanations. Another explanation could be bulk depletion from surface partitioning, which was predicted in this work to impact the Köhler growth curves for NAFA particles also at much earlier stages than at the critical point of activation. The influence of surface partitioning and reduced surface tension on the shape of Köhler curves at supersaturated conditions prior to the critical point of droplet activation has also been noted by Ruehl et al. (2016) and Davies et al. (2019).

The range of observations made for complex aerosol aerosol mixtures as well as for different model compounds suggests that surface activity is likely to be manifest in a variety of ways for atmospheric aerosols and highly dependent on both ambient conditions and particle properties, including size and chemical mixing state, as well as surface activity and intrinsic hygroscopicity of the mixture. In the present work, comparison of different surfactant representations and their performance with respect to experimentally determined CCN activity for NAFA particle mixtures suggests that conditions favoring reduced surface tension despite strong bulk depletion are mainly present in the most concentrated droplets. Such highly concentrated droplet states are seen for particles with the higher fractions of the surface active NAFA component, at the earliest stages of droplet growth, and for the smaller particles also extending to the point of activation. Using a cloud parcel model, Lowe et al. (2019) similarly found that predictions of cloud microphysics and climate radiative forcing are sensitive to organic surface properties in pristine environments with ultrafine particle sources. The NUM particles observed by Ovadnevaite et al. (2017) are typically also significantly smaller than particle sizes considered in this work. Concentrations in the droplet bulk may generally be higher for more moderately strong surfactants, which are *not* fully depleted due to surface partitioning, For example, the dicarboxylic acids (Ruehl et al., 2016), organosulfates (Hansen et al., 2015), α-pinene SOA (George et al., 2009; Ruehl et al., 2016) and pollen extracts (Prisle et al., 2019) are typically less surface active and more hygroscopic than NAFA. In these systems, the droplet state and CCN activation behavior is expected to be more sensitive to bulk/surface partitioning, as the droplet grows and A/V changes, and in response to variations in organic–inorganic interactions with changing mixing state.

When the position of the partitioning equilibrium is highly sensitive to changes in conditions, a comprehensive model is needed to fully capture variations in the droplet state with particle size and composition and in response to droplet growth and dilution. For strongly surface active mixtures with low intrinsic hygroscopicity, such as those with low solubility or very high mean molar mass similar to NAFA, both the simple partitioning representation (S) and the basic Köhler model (K) may represent CCN activity well, whereas mixtures with higher intrinsic hygroscopicity, which are typically also more moderately surface active, are likely more sensitive to the partitioning between surface and bulk and therefore less well represented by the simple models (S) and (K). This is further supported by our sensitivity analyses to average molar mass of the surface active mixture and presence of hygroscopic impurities. Thermodynamically consistent predictive modeling using independently derived mixture-specific model parameters will be needed for a wide range of atmospherically relevant aerosol systems to firmly establish which features are driving the impact of surface activity in cloud microphysics under various ambient conditions.

3.4.3 Other bulk/surface partitioning models

Several bulk/surface partitioning models have been presented and deployed in Köhler calculations to predict CCN activity for surface active aerosol systems. These models are based on different assumptions and forms of thermodynamic information and therefore it is not immediately possible to quantitatively compare their performance for a common aerosol system under identical conditions. Common for the partitioning models is that bulk and surface phases of a growing solution droplet with changing A/V are connected *via* a composition-dependent surface tension equation of state and an adsorption isotherm for the surface active components. With choice of specific equations and input parameters, each model is tailored to capture certain properties of the surface active component and has been successfully applied to describe cloud droplet activation of selected surface active aerosol mixtures. However, the different models have so far only been applied for a limited set of aerosol systems and in general models do not fully capture all interactions of surface active solute across varying droplet states. For example, the performance of our present model is seen to be somewhat reduced against experimental CCN activity for the smallest particles with highest fractions of NAFA, exactly for the conditions where the predicted partitioning equilibrium is highly sensitive to small variations in droplet state. Curiously, several studies (Ruehl et al., 2016; Ovadnevaite et al., 2017; Davies et al., 2019) note how a simplified version of the model in question performs equally well against experimental data as the full model, as was also seen here for the simple models (S).

Ruehl et al. (2016) used the "compressed film" model of Jura and Harkins (1946) to predict partitioning of surfactants into an organic surface layer. They present measured Köhler curves, in the form of growing droplet size with supersaturation, consistent with significantly reduced droplet surface tension prior to activation. Using a surface-composition based surface tension equation, Ruehl et al. (2016) find a quite different surface tension variation with growing droplet size than seen with the Szyszkowski-type equation in this work. However, their study also involves particles comprising moderately surface active dicarboxylic acids and α-pinene SOA quite different characteristics, compared to the strongly surface active NAFA mixtures. Furthermore, Ruehl et al. (2016) use a constant organic hygroscopicity parameter (Petters and Kreidenweis, 2007) and therefore do not include effects of concentration-dependent non-ideal solute interactions, which could also lead to differences in predicted water activity and droplet state, compared to the present work. In order to obtain the necessary surface tension and adsorption parameters, the model of Ruehl et al. (2016) is first fitted to the droplet size–water saturation data being described and therefore analytical, rather than predictive. As such, it would be interesting to explore the potential variation of the fitted model parameters across different conditions and in particular for droplet systems of different dimensions.

Ruehl et al. (2016) found that droplet activation typically occurs after the droplet has reached a state where all surface active solute is partitioned to the droplet surface, but the total amount is still less than what is necessary to reach the minimum surface concentration, expressed *via* the parameter δ_{org} (interpreted as a minimum surface thickness), that enables full surface coverage and reduced surface tension. In this "gaseous film" region, the model of Ruehl et al. (2016) describes essentially the same conditions as the simple partitioning model (S) by Prisle et al. (2011) and these observations are analogous to those for the Gibbs (P) and simple (S) partitioning models the present work and by Prisle et al. (2010, 2011).

The liquid-liquid phase separation (LLPS) model of Ovadnevaite et al. (2017) describes the partitioning equilibrium between separate aqueous and organic compartments assumed to represent the droplet bulk and surface, respectively. Partitioning is evaluated with considerations of composition-dependent solution non-ideality using the well-established AIOMFAC model. Where both the full and simple partitioning models of the present work and the model of Ruehl et al. (2016) in the "compressed film" region consider the surface to be comprised exclusively of the surface active component, the LLPS model accounts for presence of small amounts of organic in the aqueous phase, as well as water and water-soluble components in the organic phase. Ovadnevaite et al. (2017) evaluate droplet surface tensions from an empirical mixing rule, based on the volume-weighed composition of the organic (surface) phase. Predictive Köhler calculations are enabled for partially resolved aerosol mixtures by assuming well-defined proxies with interaction parameters described by AIOMFAC to represent both organic and inorganic aerosol components. This approach has inherent uncertainties related to the choice of proxy system and how well it represents the variation of solute-solvent and solute-solute interactions across droplet states spanned during growth and activation. As discussed by Prisle et al. (2012a), properties of a too simple proxy mixture may be more sensitive to variations in droplet state than a complex mixture.

The proxy mixture used by Ovadnevaite et al. (2017) appears to comprise components which are less surface active than the NAFA system studied here. In the Gibbs–Szyszkowski partitioning representation (P), this would entail less strong depletion from the droplet bulk phase due to surface adsorption and thus higher likelihood of (moderately) reduced droplet surface tension, including at the point of droplet activation. The particles representing so-called NUM events observed by Ovadnevaite et al. (2017) are of similar sizes as some of the smallest particle sizes studied in the present work, which activate for smaller growth factors, corresponding to more concentrated solutions, where surface tension is indeed more likely to be reduced, even in the presence of bulk depletion from surface adsorption. Similarly to the simple partitioning model of Prisle et al. (2011) and the gaseous film model of Ruehl et al. (2016), the simplified "complete phase-separation" model of Ovadnevaite et al. (2017) also assumes that surface active components are fully partitioned to the droplet surface. However, composition-dependent reduced surface tension is still considered based on the fractional coverage of the droplet surface, using the volume-based mixing rule.

In the model of Malila and Prisle (2018), partitioning occurs between the droplet bulk and a surface monolayer of finite thickness. The partitioning equilibrium is evaluated according to an extension of the semi-empirical mixing rule by Laaksonen and Kulmala (1991) yielding a surface-composition dependent solution surface tension matching the surface tension established for the corresponding bulk-composition. Similarly to the LLPS model of Ovadnevaite et al. (2017), the monolayer partitioning model allows for partitioning of all droplet components between both bulk and surface phases. However, instead of assuming a proxy solution mixture, effects of non-ideality are accounted for by using experimentally-based composition-dependent solution properties, similarly to the present framework. The monolayer model has been found to predict lower droplet surface tensions than the Gibbs models, because the surface partitioning factor $m_{\mathrm{sft}}^{S}/m_{\mathrm{sft}}^{B}$ at a given droplet size is restricted to a finite value by the volume of the surface monolayer, leading to less strong depletion of the droplet bulk. This enhances the potential predicted impact of reduced surface tension also at the point of droplet activation (Malila and Prisle, 2018; Lin et al., 2018, 2020; Bzdek et al., 2020).

Gibbs adsorption with Szyszkowski-type surface tension equations have been the most widely used in Köhler models, however, the present framework is to our knowledge the first to apply this approach on a mass-basis, allowing for thermodynamically consistent modeling of complex, chemically unresolved surface active aerosol. A significant advantage of the present model is that it is fully predictive and take non-ideal interactions in droplets into account via continuous parametrizations independently constrained by measurements. No additional parameters are introduced in the framework. A remaining disadvantage related to use of the model is that while water activity and surface tension can be accurately measured with standard instrumentation, these experiments require significant amounts of sample material to obtain a sufficient number of data points to construct robust continuous multi-dimensional parametrizations. This may pose a challenge related to ambient aerosol samples, especially for ultrafine particles sampled in pristine environments.

3.4.4 Dynamic surface tension effects

The applicability of partitioning models for CCN measurements has occasionally been questioned, due to the long equilibration times of surface tension in some (macroscopic) systems (Noziere et al., 2014; Fainerman et al., 2002; Wen et al., 1998; Coltharp and Franses, 1996; Van den Bogaert and Joos, 1980, 1979) compared to particle and droplet residence times in commonly used cloud condensation nucleus counters (Prisle et al., 2008; Kristensen et al., 2014). Recently, Lin et al. (2020) presented a detailed analysis of the effects of using surface tension parametrizations corresponding to different equilibration time scales in Köhler calculations. They observe complex relations between the influence of changing droplet size and composition, surface adsorption, and time-evolving surface tension. A clear progression of predicted surface adsorption in droplets is seen, as expected, when using surface tension parametrizations corresponding to successively longer equilibration times, but the effects of this surface adsorption on the individual Kelvin and Raoult terms of the droplet growth curve nearly cancel at every time step. We are currently not aware of any experiment that would allow verification of these predictions and only of this single existing comprehensive surface tension data set to enable similar calculations with considerations of time-evolution of bulk/surface partitioning in connection with CCN activation, therefore the general nature of such dynamic phenomena is currently unclear.

3.4.5 Large-scale applications

Thermodynamically consistent, comprehensive droplet partitioning models are generally not suitable or computationally feasible for applications to large-scale simulations (Prisle et al., 2012a; Lowe et al., 2019). Several of the frameworks described above have been presented in simplified versions, subject to various approximations. Raatikainen and Laaksonen (2011) presented an analytical solution to the Gibbs adsorption model applicable to droplets comprising a single surface active substance and ignoring all droplet solution non-idealities. Alternatively, the simple partitioning model (Prisle et al., 2011) is a phenomenological representation to emulate the CCN activation behavior of a strongly surface active component or potentially unresolved mixture which assumes complete surface partitioning and no surface tension or water activity reduction by the surface active component. The gaseous film model (Ruehl et al., 2016) and complete liquid-liquid phase separation (CLLPS) model (Ovadnevaite et al., 2017; Davies et al., 2019) both similarly assume complete surface partitioning, but where the gaseous film model also assumes surface tension equal to that of pure water, the CLLPS model captures droplet surface tension by representing surface active components with a well-known proxy mixture according to a simple mixing rule. Both the simple partitioning (S) and CLLPS models also allow for a predictive representation of droplet solution non-ideality from solute species other than the surface active components with thermodynamic relations.

The simple partitioning frameworks of Raatikainen and Laaksonen (2011) and Prisle et al. (2011) have been successfully applied in a global climate model (Prisle et al., 2012a) and that of Ovadnevaite et al. (2017) in a cloud parcel model (Lowe et al., 2019). Based on the good performance of model (S) with respect to both experimental CCN data and comprehensive calculations with the full Gibbs partitioning model for mixed NAFA–NaCl particles seen in this work, the simple representation is a promising candidate for representing effects of strong surface activity on CCN potential of other complex and unresolved organic aerosol mixtures, in particular under conditions when the partitioning is not strongly sensitive to non-ideal solute interactions in the droplets. When reduced droplet surface tension prevails, the CLLPS will likely provide a better representation of the effects of aerosol surface activity, with suitable proxy systems to describe the aerosol mixtures. Therefore, the applicability of various proxy mixtures and their ability to capture variation of surface tension across a range of droplet states must be carefully established. For conditions where effects of intrinsic hygroscopicity and non-ideal solute interactions are more prominent than surface activity and reduced surface tension of an aerosol mixture, the basic Köhler model (K) with inclusion of a suitable thermodynamic representation of droplet non-ideality may still be preferable for large-scale applications, due to its ability to represent overall CCN activity and simplicity of implementation.

4 Conclusions

We present a framework for including bulk/surface partitioning of chemically unresolved surface active aerosol components in Köhler modeling of growing droplets, using mass-based Gibbs adsorption in combination with water activity and Szyszkowski surface tension equations. The model was applied to predictive calculations of CCN activity for particles comprising chemically unresolved NAFA in mixtures with NaCl. As required input, continuous, ternary parametrizations of surface tension and water activity as functions of both NAFA and NaCl aqueous mass concentrations were constructed from measurements. The comprehensive, thermodynamically consistent predictions (P) were used to benchmark four alternative representations of the effect of NAFA surface activity in cloud droplet activation: (S) the simple partitioning representation proposed by Prisle et al. (2011), where NAFA is assumed to have zero intrinsic influence on both surface tension and water activity of droplets, (I) considering NAFA as a fully surface-partitioned, insoluble surfactant with fixed reduction of droplet surface tension, (B) assuming that droplets comprising NAFA and NaCl have identical properties to macroscopic bulk solutions of the same overall composition, and (K) treating NAFA and NaCl alike as regular soluble and homogeneously distributed (non-surface active) solutes.

Our calculations confirm that assuming macroscopic solution properties for activating droplets in the micron and sub-micron size range leads to gross overestimations of both thermodynamically consistent predictions and measurements of CCN activity, whereas simplified frameworks assuming complete surface partitioning and/or omitting surface tension reduction each describe comprehensive model results and experimental CCN data for NAFA–NaCl particles well. Furthermore, these simple models also give similar results as the full partitioning framework for a number of other properties calculated for growing and activating droplets. NAFA has significant surfactant strength in macroscopic aqueous solutions, but due to the very large surface-to-volume ratios of sub-micron activating droplets, the NAFA partitioning equilibrium is predicted to be strongly shifted toward the surface and the same total compositions do not lead to similar reductions in droplet surface tension as in macroscopic solutions, if any at all. NAFA has only modest influence on water activity in both macroscopic aqueous solutions and activating droplets alike, at least in part due to its high average molar mass, compared to hygroscopic salts. In sub-micron droplets, the weak intrinsic impact on water activity is further decreased by surface partitioning of NAFA.

With experimentally constrained accounts of non-ideal interactions in both water activity and NAFA surface activity, we therefore predict cloud microphysical behavior for chemically complex surface active aerosol mixtures which closely resembles that previously seen for systems comprising simple, strong surfactants with well-defined molecular properties. Contrary to other recent works, we here find that sub-micron droplet properties are governed by size-modulated influences of surface activity on both water activity and curvature terms of the Köhler curve and that the "missing Raoult effect" from bulk-phase depletion due to surface adsorption overpowers any enhancement of droplet growth and activation from decreased surface tension. We are currently not aware of any other chemically unresolved or complex aerosol system for which experimental data are available to enable a similar analysis. However, we hope that the presented framework will motivate more measurements to provide the necessary comprehensive, thermodynamically consistent characterization of CCN activity for a broader range of complex surface active aerosol systems. This will contribute significantly to clarify the conditions where cloud microphysics is governed by each of the effects of aerosol surface activity and their most suitable representation in atmospheric modeling.

Surface activity of aerosol components may also have important implications for other processes related to cloud microphysics, including aqueous droplet chemistry during cloud processing in the atmosphere. Firstly, owing to the relatively large surface areas of sub-micron droplets, aqueous surface chemistry, such as the photosensitized limonene uptake by Humic Acid, another atmospheric model HULIS mixture (Tsui and McNeill, 2018), may be significantly enhanced, compared to reactions in the bulk phase. Secondly, extensive surface partitioning will change the chemical environment and possible chemical reaction pathways and rates of surface active species in both surface (Prisle et al., 2012b; Öhrwall et al., 2015; Werner et al., 2018) and bulk phases. When depleted from the droplet bulk, these compounds will not be as readily available for reactions with soluble species in the aqueous droplet phase and the rate determining concentrations will be vastly different from a macroscopic solution with identical total composition. Thirdly, pressure-sensitive reactions in the droplet phase may be impacted by the elevated pressures inside microscopic systems from the finite curvature radii according to the Young-Laplace equation (Adamson and Gast, 1997). This pressure elevation is also the basis for the Kelvin effect and depends directly on the droplet surface tension. If the surface tension of microscopic droplets is closer to that of pure water than of a macroscopic surfactant solution, this may need to be taken into account in considerations of the yields and pathways of such reactions. A comprehensive description of both droplet bulk and surface composition, by including size-dependent surface adsorption and its response to changing ambient humidity and droplet growth, may be therefore crucial for understanding the mechanisms and predicting the extent of chemical processes in microscopic atmospheric droplets.

Author contributions. NLP conceived, planned and secured funding for the project. NLP did the model implementation and made the model calculations, analyzed all results, and wrote the first and revised versions of the manuscript and the responses to reviewers.

Competing interests. The author declares no competing interests.

Acknowledgements. The author thanks Bjarke Mølgaard for his work on the surface tension and water activity parametrizations, Silvia Calderón, Jack J. Lin, Jussi Malila, Tomi Raatikainen, Sampo Vepsäläinen, and Taina Yli-Juuti for valuable discussions and technical support, and Thomas B. Kristensen and Merete Bilde for providing measurement data previously published by Kristensen et al. (2014) and Lin et al. (2020). This project has received funding from the European Research Council (ERC) under the European Union's Horizon 2020 research and innovation programme (Project SURFACE, Grant Agreement No. 717022). N. L. Prisle also gratefully acknowledges funding from the Carlsberg Foundation (Grants 2009_01_0366 and 2010_01_0391) and Academy of Finland (Grants 257411, 308238, 314175, and 335649).

References

Adamson, A. and Gast, A.: Physical Chemistry of Surfaces, John Wiley & Sons, Inc., sixth edn., 1997.

Alvarez, N. J., Walker, L. M., and Anna, S. L.: A Microtensiometer To Probe the Effect of Radius of Curvature on Surfactant Transport to a Spherical Interface, Langmuir, 26, 13 310–13 319, https://doi.org/10.1021/la101870m, https://doi.org/10.1021/la101870m, pMID: 20695573, 2010.

Alvarez, N. J., Walker, L. M., and Anna, S. L.: A criterion to assess the impact of confined volumes on surfactant transport to liquid–fluid interfaces, Soft Matter, 8, 8917–8925, https://doi.org/10.1039/C2SM25447F, http://dx.doi.org/10.1039/C2SM25447F, 2012.

Asa-Awuku, A., Sullivan, A., Hennigan, C. J., Weber, R. J., and Nenes., A.: Investigation of molar volume and surfactant characteristics of water-soluble organic compounds in biomass burning aerosol, Atmospheric Chemistry and Physics, 8, 799–812, 2008.

Aumann, E., Hildemann, L., and Tabazadeh, A.: Measuring and modeling the composition and temperature-dependence of surface tension for organic solutions, Atmospheric Environment, 44, 329–337, 1967.

Bianco, H. and Marmur, A.: The Dependence of the Surface Tension of Surfactant Solutions on Drop Size, Journal of Colloid and Interface Science, 151, 517–522, 1992.

Bilde, M. and Svenningsson, B.: CCN Activation of Slightly Soluble Organics: The Importance of Small Amounts of Inorganic Salt and Particle Phase, Tellus, 56B, 128–134, 2004.

Booth, A. M., Topping, D. O., McFiggans, G., and Percival, C. J.: Surface tension of mixed inorganic and dicarboxylic acid aqueous solutions at 298.15 K and their importance for cloud activation predictions, Phys. Chem. Chem. Phys., 11, 8021–8028, 2009.

Bzdek, B. R., Reid, J. P., Malila, J., and Prisle, N. L.: The surface tension of surfactant-containing, finite volume droplets, Proceedings of the National Academy of Sciences, 117, 8335–8343, 2020.

Cheng, Y., Li, S.-M., Leithead, A., Brickell, P. C., and Leaitch, W. R.: Characterizations of *cis*-pinonic acid and n-fatty acids on fine aerosols in the Lower Fraser Valley during Pacific 2001 Air Quality Study, Atmospheric Environment, 38, 5789–5800, 2004.

Coltharp, K. A. and Franses, E. I.: Equilibrium and dynamic surface tension behavior of aqueous soaps: sodium octanoate and sodium dodecanoate (sodium laurate), Colloids and Surfaces A: Physicochemical and Engineering Aspects, 108, 225–242, 1996.

Davies, J. F., Zuend, A., and Wilson, K. R.: Technical note: The role of evolving surface tension in the formation of cloud droplets, Atmospheric Chemistry and Physics, 19, 2933–2946, 2019.

Dawson, K. W., Petters, M. D., Meskhidze, N., Suda Petters, S., and Kreidenweis, S. M.: Hygroscopic growth and cloud droplet activation of xanthan gum as a proxy for marine hydrogels, Journal of Geophysical Research: Atmospheres, 121, 11 803–11 818, 2016.

Dillmann, A. and Meier, G. E. A.: A refined droplet approach to the problem of homogeneous nucleation from the vapor phase, The Journal of Chemical Physics, 94, 3872–3884, https://doi.org/10.1063/1.460663, https://doi.org/10.1063/1.460663, 1991.

Dinar, E., Mentel, T. F., and Rudich, Y.: The density of humic acids and humic like substances (HULIS) from fresh and aged wood burning and pollution aerosol particles, Atmospheric Chemistry and Physics, 6, 5213–5224, 2006a.

Dinar, E., Taraniuk, I., Graber, E. R., Katsman, S., Moise, T., Anttila, T., Mentel, T. F., and Rudich, Y.: Cloud Condensation Nuclei properties of model and atmospheric HULIS, Atmospheric Chemistry and Physics, 6, 2465–2481, 2006b.

Facchini, M., Mircea, M., Fuzzi, S., and Charlson, R.: Cloud Albedo Enhancement by Surface-Active Organic Solutes in Growing Droplets, Nature, 401, 257–259, https://doi.org/10.5194/acp-10-8219-2010, 1999.

Facchini, M., Decesari, S., Mircea, M., Fuzzi, S., and Loglio, G.: Surface Tension of Atmospheric Wet Aerosol and Cloud/Fog Droplets in Relation to their Organic Carbon Content and Chemical Composition, Atmospheric Environment, 34, 4853–4857, 2000.

Fainerman, V. B., Miller, R., and Möhwald, H.: General Relationships of the Adsorption Behavior of Surfactants at the Water/Air Interface, J. Phys. Chem. B, 106, 809–819, 2002.

Forestieri, S. D., Staudt, S. M., Kuborn, T. M., Faber, K., Ruehl, C. R., Bertram, T. H., and Cappa, C. D.: Establishing the impact of model surfactants on cloud condensation nuclei activity of sea spray aerosol mimics, Atmospheric Chemistry and Physics, 18, 10 985–11 005, 2018.

Frosch, M., Prisle, N. L., Bilde, M., Varga, Z., and Kiss, G.: Joint effect of organic acids and inorganic salts on cloud droplet activation, Atmospheric Chemistry and Physics, 11, 3895–3911, https://doi.org/10.5194/acp-11-3895-2011, 2011.

George, I., Chang, R.-W., Danov, V., Vlasenko, A., and Abbatt, J.: Modification of cloud condensation nucleus activity of organic aerosols by hydroxyl radical heterogeneous oxidation, Atmospheric Environment, 43, 5038 – 5045, https://doi.org/https://doi.org/10.1016/j.atmosenv.2009.06.043, http://www.sciencedirect.com/science/article/pii/S1352231009005615, 2009.

Gérard, V., Nozière, B., Baduel, C., Fine, L., Frossard, A. A., and Cohen, R. C.: Anionic, Cationic, and Nonionic Surfactants in Atmospheric Aerosols from the Baltic Coast at Askö, Sweden: Implications for Cloud Droplet Activation, Environmental Science & Technology, 50, 2974–2982, 2016.

Gibbs, J., Bumstead, H., Longley, W., and Name, R. V.: The Collected Works of J. Willard Gibbs, Longmans, Green and Co., 1928.

Graber, E. R. and Rudich, Y.: Atmospheric HULIS: How humic-like are they? A comprehensive and critical review, Atmos. Chem. Phys., 6, 729–753, 2006.

Hansen, A. M. K., Hong, J., Raatikainen, T., Kristensen, K., Ylisirniö, A., Virtanen, A., Petäjä, T., Glasius, M., and Prisle, N. L.: Hygroscopic properties and cloud condensation nuclei activation of limonene-derived organosulfates and their mixtures with ammonium sulfate, Atmospheric Chemistry and Physics, 15, 14 071–14 089, https://doi.org/10.5194/acp-15-14071-2015, http://www.atmos-chem-phys.net/15/14071/2015/, 2015.

Harmon, C., Grimm, R., McIntire, T., Peterson, M., Njegic, B., Angel, V., Alshawa, A., Underwood, J., Tobias, D., Gerber, R., Gordon, M., Hemminger, J., and Nizkorodov, S.: Hygroscopic growth and deliquescence of NaCl nanoparticles mixed with surfactant SDS, Journal of Physical Chemistry B, 114, 2435–2449, 2010.

Hyvärinen, A.-P., Lihavainen, H., Gaman, A., Vairila, L., Ojala, H., Kulmala, M., and Viisanen, Y.: Surface Tensions and Densities of Oxalic, Malonic, Succinic, Maleic, Malic, and *cis*-Pinonic Acids, Journal of Chemical and Engineering Data, 51, 255–260, 2006.

Jin, F., Balasubramaniam, R., and Stebe, K. J.: SURFACTANT ADSORPTION TO SPHERICAL PARTICLES: THE INTRINSIC LENGTH SCALE GOVERNING THE SHIFT FROM DIFFUSION TO KINETIC-CONTROLLED MASS TRANSFER, The Journal of Adhesion, 80, 773–796, https://doi.org/10.1080/00218460490480770, https://doi.org/10.1080/00218460490480770, 2004.

Jura, G. and Harkins, W. D.: Surfaces of Solids. XIV. A Unitary Thermodynamic Theory of the Adsorption of Vapors on Solids and of Insoluble Films on Liquid Subphases, Journal of the American Chemical Society, 68, 1941–1952, 1946.

Kiss, G. and Hansson, H.-C.: Application of osmolality for the determination of water activity and the modelling of cloud formation, Atmospheric Chemistry and Physics Discussions, 4, 7667–7689, 2004.

Kiss, G., Tombacz, E., and Hansson, H.-C.: Surface Tension Effects of Humic-Like Substances in the Aqueous Extract of Tropospheric Fine Aerosol, Journal of Atmospheric Chemistry, 50, 279–294, 2005.

Köhler, H.: The Nucleus in and the Growth of Hygroscopic Droplets, Transactions of the Faraday Society, 32, 1152–1161, 1936.

Kristensen, T. B., Prisle, N. L., and Bilde, M.: Cloud droplet activation of mixed model HULIS and NaCl particles: Experimental results and κ-Köhler theory, Atmospheric Research, 137, 167–175, 2014.

Kroflič, A., Frka, S., Simmel, M., Wex, H., and Grgić, I.: Size-resolved surface active substances of atmospheric aerosol: reconsideration of the impact on cloud droplet formation, Environmental Science & Technology, 0, null, https://doi.org/10.1021/acs.est.8b02381, https://doi.org/10.1021/acs.est.8b02381, pMID: 30048123, 2018.

Laaksonen, A.: The Composition Size Dependence of Aerosols Created by Dispersion of Surfactant Solutions, Journal of Colloid and Interface Science, 159, 517–519, 1993.

Laaksonen, A. and Kulmala, M.: An explicit cluster model for binary nuclei in water–alcohol systems, The Journal of Chemical Physics, 95, 6745–6748, 1991.

Lee, B.-B., Chan, E.-S., Ravindra, P., and Khan, T. A.: Surface tension of viscous biopolymer solutions measured using the du Nouy ring method and the drop weight methods, Polymer Bulletin, 69, 471–489, 2012.

Li, Z., Williams, A., and Rood, M.: Influence of Soluble Surfactant Properties on the Activation of Aerosol Particles Containing Inorganic Solute, Journal of the Atmospheric Sciences, 55, 1859–1866, 1998.

Lin, J. J., Malila, J., and Prisle, N. L.: Cloud droplet activation of organic–salt mixtures predicted from two model treatments of the droplet surface, Environmental Science: Processes & Impacts, 20, 1611–1629, 2018.

Lin, J. J., Kristensen, T. B., Calderón, S. M., Malila, J., and Prisle, N. L.: Effects of surface tension time-evolution for CCN activation of a complex organic surfactant, Environmental Science: Processes & Impacts, 22, 271–284, 2020.

Low, R.: A Theoretical Study of Nineteen Condensation Nuclei, Journal de Recherches Atmospheriques, pp. 65–78, 1969.

Lowe, S. J., Partridge, D. G., Davies, J. F., Wilson, K. R., Topping, D., and Riipinen, I.: Key drivers of cloud response to surface-active organics, Nature Communications, 10, 1–12, 2019.

Mäkelä, J. and Manninen, P.: Molecular size distribution od structure investigations of humic substances in groundwater, working report 2008-36, Posiva Oy, Posiva Oy, Olkiluoto, FI-27160 Eurajoki, Finland, 2008.

Malila, J. and Prisle, N. L.: A monolayer partitioning scheme for droplets of surfactant solutions, Journal of Advances in Modeling Earth Systems, 10, 3233–3251, 2018.

Meissner, H. P. and Michaels, A. S.: Surface Tensions of Pure Liquids and Liquid Mixtures, Industrial & Engineering Chemistry, 41, 2782–2787, https://doi.org/10.1021/ie50480a028, https://doi.org/10.1021/ie50480a028, 1949.

Mochida, M., Kitamori, Y., Kawamura, K., Nojiri, Y., and Suzuki, K.: Fatty acids in the marine atmosphere: Factors governing their concentrations and evaluation of organic films on sea-salt particles, Journal of Geophysical Research, 107, D17S4325, https://doi.org/10.1029/2001JD001278, 2002.

Mochida, M., Kawamura, K., Umemoto, N., Kobayashi, M., Matsunaga, S., Lim, H.-J., Turpin, B., Bates, T., and Simoneit, B.: Spatial distributions of oxygenated organic compounds (dicarboxylic acids, fatty acids, and levoglucosan) in marine aerosols over the western Pacific and off the coast of East Asia: Continental outflow of organic aerosols during the ACE-Asia campaign, Journal of Geophysical Research, 108, D23S8638, https://doi.org/10.1029/2002JD003249, 2003.

Noziere, B., Baduel, C., and Jaffrezo, J.-L.: The dynamic surface tension of atmospheric aerosol surfactants reveals new aspectsof cloud activation, Nature Communications, 5, 1–7, 2014.

Öhrwall, G., Prisle, N. L., Ottosson, N., Werner, J., Ekholm, V., Walz, M.-M., and Björneholm, O.: Acid–Base Speciation of Carboxylate Ions in the Surface Region of Aqueous Solutions in the Presence of Ammonium and Aminium Ions, The Journal of Physical Chemistry B, 119, 4033–4040, 2015.

Ovadnevaite, J., Zuend, A., Laaksonen, A., Sanchez, K. J., Roberts, G., Ceburnis, D., Decesari, S., Rinaldi, M., Hodas, N., Facchini, M. C., Seinfeld, J. H., and O' Dowd, C.: Surface tension prevails over solute effect in organic-influenced cloud droplet activation, Nature, 546, 637–641, 2017.

Petters, M. and Kreidenweis, S.: A single parameter representation of hygroscopic growth and cloud condensation nucleus activity–Part 3: Including surfactant partitioning, Atmos. Chem. Phys., 13, 1081–1091, 2013.

Petters, M. D. and Kreidenweis, S. M.: A single parameter representation of hygroscopic growth and cloud condensation nucleus activity, Atmos. Chem. Phys., 7, 1961–1971, 2007.

Petters, S. S. and Petters, M. D.: Surfactant effect on cloud condensation nuclei for two-component internally mixed aerosols, Journal of Geophysical Research: Atmospheres, 121, 2016.

Poulain, L., Wu, Z., Petters, M. D., Wex, H., Hallbauer, E., Wehner, B., Massling, A., Kreidenweis, S. M., and Stratmann, F.: Towards closing the gap between hygroscopic growth and CCN activation for secondary organic aerosols - Part 3: Influence of the chemical composition on the hygroscopic properties and volatile fractions of aerosols, Atmos. Chem. Phys., 10, 3775–3785, 2010.

Prisle, N.: Cloud Condensation Nuclei Properties of Organic Aerosol Particles: Effects of Acid Dissociation and Surfactant Partitioning, M.Sc. Thesis, Department of Chemistry, Faculty of Science, University of Copenhagen, 2006.

Prisle, N. L., Raatikainen, T., Sorjamaa, R., Svenningsson, B., Laaksonen, A., and Bilde, M.: Surfactant partitioning in cloud droplet activation: a study of C8, C10, C12 and C14 normal fatty acid sodium salts, Tellus, 60B, 416–431, https://doi.org/10.1111/j.1600-0889.2008.00352.x, 2008.

Prisle, N. L., Raatikainen, T., Laaksonen, A., and Bilde, M.: Surfactants in cloud droplet activation: mixed organic-inorganic particles, Atmos. Chem. Phys., 10, 5663–5683, https://doi.org/10.5194/acp-10-5663-2010, 2010.

Prisle, N. L., Dal Maso, M., and Kokkola, H.: A simple representation of surface active organic aerosol in cloud droplet formation., Atmos. Chem. Phys., 11, 4073–4083, https://doi.org/10.5194/acp-11-4073-2011, 2011.

Prisle, N. L., Asmi, A., Topping, D., Partanen, A.-I., Romakkaniemi, S., Dal Maso, M., Kulmala, M., Laaksonen, A., Lehtinen, K. E. J., McFiggans, G., and Kokkola, H.: Surfactant effects in global simulations of cloud droplet activation., Geophys. Res. Lett., 39, L05 802, https://doi.org/10.1029/2011GL050467, 2012a.

Prisle, N. L., Ottosson, N., Öhrwall, G., Söderström, J., Maso, M. D., and Björneholm, O.: Surface/bulk partitioning and acid/base speciation of aqueous decanoate: direct observations and atmospheric implications., Atmos. Chem. Phys., 12, 12 227–12 242, https://doi.org/10.5194/acp-12-12227-2012, 2012b.

Prisle, N. L., Lin, J. J., Purdue, S., Lin, H., Meredith, J. C., and Nenes, A.: Cloud condensation nuclei activity of six pollenkitts and the influence of their surface activity, Atmospheric Chemistry and Physics, 19, 4741–4761, 2019.

Raatikainen, T. and Laaksonen, A.: A simplified treatment of surfactant effects on cloud drop activation, Geosci. Model Dev., 4, 107–116, https://doi.org/10.5194/gmd-4-107-2011, 2011.

Rood, M. J. and Williams, A. L.: Reply, Journal of the Atmospheric Sciences, 58, 1468–1473, 2001.

Ruehl, C. R., Chuang, P. Y., and Nenes, A.: Aerosol hygroscopicity at high (99 to 1001329–1344, https://doi.org/10.5194/acp-10-1329-2010, http://www.atmos-chem-phys.net/10/1329/2010/, 2010.

Ruehl, C. R., Davies, J. F., and Wilson, K. R.: An interfacial mechanism for cloud droplet formation on organic aerosols, Science, 351, 1447–1450, https://doi.org/10.1126/science.aad4889, http://science.sciencemag.org/content/351/6280/1447, 2016.

Shulman, M., Jacobson, M., Charlson, R., Synovec, R., and Young, T.: Dissolution Behavior and Surface Tension Effects of Organic Compounds in Nucleating Cloud Droplets, Geophysical Research Letters, 23, 277–280, 1996.

Sorjamaa, R., Svenningsson, B., Raatikainen, T., Henning, S., Bilde, M., and Laaksonen, A.: The Role of Surfactants in Köhler Theory Reconsidered, Atmospheric Chemistry and Physics, 4, 2107–2117, 2004.

Topping, D.: An analytical solution to calculate bulk mole fractions for any number of components in aerosol droplets after considering partitioning to a surface layer, Geoscientific Model Development, 3, 635–642, https://doi.org/10.5194/gmd-3-635-2010, http://www.geosci-model-dev.net/3/635/2010/, 2010.

Tsui, W. G. and McNeill, V. F.: Modeling Secondary Organic Aerosol Production from Photosensitized Humic-like Substances (HULIS), Environmental Science & Technology Letters, 5, 255–259, https://doi.org/10.1021/acs.estlett.8b00101, https://doi.org/10.1021/acs.estlett.8b00101, 2018.

Van den Bogaert, R. and Joos, P.: Dynamic surface tensions of sodium myristate solutions, The Journal of Physical Chemistry, 83, 2244–2248, 1979.

Van den Bogaert, R. and Joos, P.: Diffusion-controlled adsorption kinetics for a mixture of surface active agents at the solution-air interface, The Journal of Physical Chemistry, 84, 190–194, 1980.

Vanhanen, J., Hyvärinen, A.-P., Anttila, T., Raatikainen, T., Viisanen, Y., and Lihavainen, H.: Ternary solution of sodium chloride, succinic acid and water; surface tension and its influence on cloud droplet activation, Atmospheric Chemistry and Physics, 8, 4595–4604, 2008.

Varga, Z., Kiss, G., and Hansson, H.-C.: Modelling the cloud condensation nucleus activity of organic acids on the basis of surface tension and osmolality measurements, Atmospheric Chemistry and Physics, 7, 4601–4611, 2007.

Walz, M.-M., Werner, J., Ekholm, V., Prisle, N. L., Ohrwall, G., and Bjorneholm, O.: Alcohols at the aqueous surface: chain length and isomer effects, Phys. Chem. Chem. Phys., 18, 6648–6656, https://doi.org/10.1039/C5CP06463E, http://dx.doi.org/10.1039/C5CP06463E, 2016.

Wen, X. Y., McGinnis, K. C., and Franses, E. I.: Unusually low dynamic surface tensions of aqueous solutions of sodium myristate, Colloids and Surfaces A: Physicochemical and Engineering Aspects, 143, 371–380, 1998.

Werner, J., Julin, J., Dalirian, M., Prisle, N. L., Öhrwall, G., Persson, I., Björneholm, O., and Riipinen, I.: Succinic acid in aqueous solution: connecting microscopic surface composition and macroscopic surface tension, Phys. Chem. Chem. Phys., pp. –, https://doi.org/10.1039/C4CP02776K, http://dx.doi.org/10.1039/C4CP02776K, 2014.

Werner, J., Persson, I., Björneholm, O., Kawecki, D., Saak, C.-M., Walz, M.-M., Ekholm, V., Unger, I., Valtl, C., Caleman, C., Öhrwall, G., and Prisle, N. L.: Shifted equilibria of organic acids and bases in the aqueous surface region, Physical Chemistry Chemical Physics, 20, 23 281–23 293, 2018.

Wex, H., Hennig, T., Salma, I., Ocskay, R., Kiselev, A., Henning, S., Massling, A., Wiedensohler, A., and Stratmann, F.: Hygroscopic growth and measured and modeled critical supersaturations of an atmospheric HULIS sample, GEOPHYSICAL RESEARCH LETTERS, 34, L02 818, https://doi.org/10.1029/2006GL028260, 2007.

Yassaa, N., Meklati, B. Y., Cecinato, A., and Marino, F.: Particulate n-alkanes, n-alkanoic acids and polycyclic aromatic hydrocarbons in the atmosphere of Algiers City Area, Atmospheric Environment, 35, 1843–1851, 2001.

Zamora, I. R. and Jacobson, M. Z.: Measuring and modeling the hygroscopic growth of two humic substances in mixed aerosol particles of atmospheric relevance, Atmos. Chem. Phys., 13, 8973–8989, https://doi.org/10.5194/acp-13-8973-2013, 2013.